

**CAVITY NATURAL CONVECTION OF ZINC OXIDE-
WATER NANOFLUID – EXPERIMENTAL WORK**

by

KYOUNG-YEOLL (JOHN) LEE

Submitted in partial fulfilment of the requirements for the degree

MASTER OF ENGINEERING

in the

Faculty of Engineering, Built Environment and Information Technology

University of Pretoria

2015

Abstract

Title : Cavity natural convection of zinc oxide-water nanofluid – experimental work

Supervisor : Dr M Sharifpur

Co-supervisor : Prof JP Meyer

Department : Mechanical and Aeronautical Engineering

University : University of Pretoria

Degree : Master of Engineering (Mechanical Engineering)

Nanofluids show great potential for conventional heat transfer fluids that could benefit industries and save huge costs. Nanofluids are well known for enormously enhancing the thermal conductivity of a base fluid. However, there is a lack of consensus in experimental and numerical results for the natural convection heat transfer of nanofluids in a closed cavity. In this study, the cavity flow natural convection of zinc oxide (ZnO)-water is investigated experimentally. The ZnO nanoparticles have an average size of 20 nm and the nanofluids were prepared with different volume fractions of 0.09, 0.18, 0.36, 0.5 and 1 volume percentage (vol.%) (0.5, 1, 2, 3 and 5.67 weight percentage). The stability of the ZnO nanofluid is verified using a spectrophotometer and zeta potential measurement at various temperatures and concentrations of the nanofluids. Zeta potential values are measured within the stable range, and no sedimentation of nanoparticles is indicated within 24 hours. The viscosity of ZnO-water nanofluid is also measured experimentally, which is 20% higher than the use of the traditional Einstein viscosity model at 1 vol.%. The heat transfer efficiency of natural convection of ZnO-water nanofluid is examined experimentally in a closed square cavity at a Rayleigh number (Ra) range between $7.9E+7$ and $8.9E+8$. The cavity is heated vertically from one vertical wall and cooled from the opposite wall. Other sides, including top and bottom walls, are insulated to be adiabatic. Consequently, the suspension of ZnO nanoparticles in water does not enhance the natural convection heat transfer coefficient. The systematic deterioration of the natural convection heat transfer coefficient is observed as increasing in the concentration of nanoparticles.

Keywords: *Nanofluids, natural convection, thermophysical properties of nanofluids, experimental, ZnO, cavity flow*

Acknowledgements

Firstly, I would like to acknowledge God for everything that was provided to me to complete this work.

I express my profound gratitude to my supervisor, Dr Sharifpur, for offering his technical knowledge, support and guidance throughout the research. I would like to thank Prof Meyer for giving me the opportunity to conduct research in an environment with excellent facilities and knowledgeable staff.

I would also like to thank my parents, as well as my brother and sister, for their moral support throughout my education.

Lastly, I would also like to thank the University of Pretoria and the National Research Foundation (NRF) for their financial support.

Table of contents

Abstract.....	i
Acknowledgements.....	ii
Table of contents.....	iii
List of figures.....	vi
List of tables.....	viii
Nomenclature.....	ix
1. Introduction.....	1
1.1 Background.....	1
1.2 Problem statement.....	2
1.3 Aim.....	2
1.4 Objective.....	2
1.5 Scope of work.....	3
1.6 Overview of dissertation.....	3
2. Literature study.....	4
2.1 Introduction.....	4
2.2 Formulation method for nanofluids.....	4
2.2.1 One-step method.....	4
2.2.2 Two-step method.....	4
2.2.3 Surfactant.....	5
2.3 Stability of nanofluids.....	7
2.3.1 Zeta potentials analysis.....	7

2.3.2 Spectral absorbency analysis	8
2.3.3 Sedimentation	8
2.4 General applications of nanofluids	8
2.5 Thermal conductivity	10
2.5.1 Thermal conductivity of ZnO-water nanofluids	12
2.6 Viscosity of nanofluids	13
2.7 The specific heat, density and thermal expansion coefficient of nanofluid	14
2.8 Natural convection of nanofluids	15
2.9 Summary and conclusion	20
3. Method	22
3.1 Introduction	22
3.2 Nanofluids	22
3.2.1 Formulating nanofluids	22
3.2.2 Stability of nanofluid: zeta potential	24
3.2.3 Stability of nanofluid: spectrophotometer	26
3.3 Experiment method	28
3.3.1 Heat exchanger and cavity design	28
3.3.2 Test section	30
3.3.3 Experimental setup and procedure	33
3.4 Physical configuration and formula	38
3.5 Summary and conclusion	40
4. Result	41

4.1 Introduction.....	41
4.2 Non-dimensional temperature versus non-dimensional distance.....	41
4.3 Effect of volume fraction and temperature on the viscosity of ZnO-water nanofluids.....	42
4.4 Heat transfer coefficient for different mass fractions of ZnO-water nanofluid	45
4.5 The effect of changing ZnO-water nanofluids' Ra on Nu with different mass fraction	46
4.6 Uncertainty analysis.....	46
5. Conclusion	48
References.....	49
Appendix A – Cavity design.....	59
Appendix B – Viscosity of ZnO-water nanofluid	62
Appendix C – Ra, Nu and heat transfer coefficient data.....	67
Appendix D – Uncertainty calculation.....	68

List of figures

Figure 1: Effects of thermal conductivity and pumping power on heat transfer [1].....	10
Figure 2: TEM image of ZnO-water nanofluid (a); and scanning electron microscopy (SEM) image of a dry powder of ZnO particles (b).....	23
Figure 3: The effect of the sonication energy density of an average aggregation size on ZnO-water nanofluid [45].....	24
Figure 4: A stability plot of zeta potential versus pH [19].....	25
Figure 5: The influence of temperature on the zeta potential value of a ZnO-water nanofluid with a 0.06 vol.% concentration	26
Figure 6: Absorbance of 0.0018 vol.% ZnO-water nanofluid versus wavelength	27
Figure 7: The effect of time on the concentration of ZnO-water	28
Figure 8: Heat exchanger (a) and solid work design of heat exchanger (b).....	29
Figure 9: Cavity design by solid work (a), its section view (b) and the actual cavity (c).....	30
Figure 10: Sketch of the experiment test section and thermocouple location.....	31
Figure 11: A schematic diagram of the experimental setup.....	33
Figure 12: A schematic representation of a cavity problem for the natural convection flow, together with the relevant notation and boundary condition.....	38
Figure 13: The non-dimensional temperature versus the non-dimensional distance in the cavity	41
Figure 14: The effect of volume fraction and temperature on the viscosity of ZnO-water nanofluid ..	43
Figure 15: The viscosity of a ZnO nanofluid with theoretical and experimental measurements.....	44
Figure 16 : The heat transfer coefficient for the different volume fractions of a ZnO nanofluid at various temperature differences between the hot and cold walls.....	45
Figure 17 : The effect of a changing ZnO-water nanofluid's Ra on the Nu with a different volume fraction	46

Figure A. 1: Test section dimensional drawings.....	60
Figure A. 2: Test section drawing with bill of materials.....	61
Figure B. 1: Viscosity of ZnO-water with 0% concentration as a function of temperature.....	63
Figure B. 2: Viscosity of ZnO-water with 0.09% concentration as a function of temperature.....	64
Figure B. 3: Viscosity of ZnO-water with 0.18% concentration as a function of temperature.....	64
Figure B. 4: Viscosity of ZnO-water with 0.36% concentration as a function of temperature.....	65
Figure B. 5: Viscosity of ZnO-water with 0.5% concentration as a function of temperature.....	65
Figure B. 6: Viscosity of ZnO-water with 1% concentration as a function of temperature.....	66

List of tables

Table 1: Surfactants used for nanofluid stability	6
Table 2 : Application of nanofluids and description of the filed of potential application	9
Table 3: The thermal conductivity of a ZnO-water nanofluid	13
Table 4: Thermophysical properties of water fluid and ZnO [61]	15
Table 5: Previous research for the natural convection of nanofluid in a closed rectangular cavity	18
Table 6: The effect of different concentrations on zeta potential of ZnO-water nanofluids	25
Table 7: Thermocouple location	32
Table 8: Experiment procedure	35
Table B. 1: Viscosity of ZnO-water with volume concentration of (a) 0%, (b) 0.09%, (c) 0.18%, (d) 0.36%, (e) 0.5% and (f) 1%	62
Table C. 1: Ra, Nu and heat transfer coefficient data	67

Nomenclature

Ag	Silver
Al ₂ O ₃	Aluminium oxide
Au	Gold
C _p	Specific heat, J/(kgK)
CTAB	Cetyl trimethyl ammonium bromide
Cu	Copper
CuO	Copper oxide
EG	Ethylene glycol
Gr	Grashof number
g	Acceleration due to gravity, m/s ²
h	Heat transfer coefficient, W/(m ² .K)
k	Thermal conductivity, W/(m.K)
L _c	Characteristic length of cavity, m
MWCNT	Multi-walled carbon nanotubes
NRF	National Research Foundation
P	Pressure, Pa
PAA	Polyacrylic acid
SDBS	Sodium dodecylbenzene sulfonate
SDS	Sodium dodecyl sulphate
SEM	Scanning electron microscopy
SIMPLER	Semi-implicit method for pressure-linked equations – revised
SiO	Silicon oxide
SWCNT	Single-walled carbon nanotubes
TAHP	Tetramethylammonium hydroxide pentahydrate

T_{ave}	Average temperature in the cavity
T_C	Temperature of the cold wall in the cavity
TEM	Transmission electron microscopy
T_H	Temperature of the hot wall in the cavity
T_{in}	Temperatures at the inlet of the heat exchanger
T_{out}	Temperatures at the outlet of the heat exchanger
T_{ave}	Average temperatures of the hot and cold walls
Ti_2O	Titanium oxide
x	Distance along the cavity from hot wall, m
TMAH	Tetramethylammonium hydroxide
ZnO	Zinc oxide
ZP	Zeta potential, mV
ZrO_2	Zirconium dioxide

Dimensionless parameters

Nu	Nusselt number
Pr	Prandtl number
Ra	Rayleigh number
θ	Non-dimensional temperature, K

Greek symbols

α	Thermal diffusivity, m^2/s
β	Volumetric coefficient of thermal expansion, $1/K$
ε	Heat transfer coefficient ratio
ϕ	Volume fraction of nanofluid
μ	Dynamic viscosity, $kg/m.s$
ν	Kinematic viscosity, $\rho f / \rho f$

ρ Density, kg/m^3
 δ Non-dimensional distance of the cavity

Subscripts

bf Base fluid
eff Effective
nf Nanofluid
np Nanoparticle

1. Introduction

1.1 Background

Over the last century, many researchers interested in industrial and electronic cooling processes have paid attention to efficient methods of heat transfer. The higher the heat transfer coefficient (W/m^2K), the more efficient the system's power output. Therefore, a new class of heat transfer mediums with higher heat transfer performance has been investigated. The innovative method of enhancing heat transfer, which was introduced by Choi [1], is to disperse nano-sized (1 to 100 nm) metallic, metal oxide or polymeric particles in conventional heat transfer fluids.

The latest technology has the ability to fabricate nanoparticles that can be dispersed easily without rapid settling in the base fluid. To achieve thermal and cost-efficient conventional heat transfer fluids, nanofluids seem to be an alternative solution to suitably meet technological demands in many industries, such as solar collectors, nuclear reactor cooling, electronic cooling, automobiles, chemical processes and building air conditioning [2].

Sharifpur, Ntumba and Meyer [3] reported the parametric evaluation of effective thermal conductivity, and Sharifpur, Ntumba and Meyer [4] reported on the viscosity of nanofluids. As a result, it is concluded that nanofluids enhance the thermal properties of the base fluid significantly with low volume concentration. However, it is uncertain that nanofluids will increase the heat transfer coefficient in forced or natural convection (while the viscosity increases as well). Nanofluid systems are complex and there is still disagreement among researchers about nanofluids' heat transfer efficiency. It is crucial to determine which nanofluids may enhance or deteriorate the heat transfer coefficient because industries will not consider using nanofluid as a heat transfer fluid if the heat transfer coefficient is decreased by

adding nanoparticles in the coolant.

1.2 Problem statement

Nanofluids show great potential for conventional heat transfer. Many numerical and theoretical studies report that nanofluids enhance the heat transfer performance of base fluids in natural convection. However, scientists still dispute whether nanofluids can benefit heat transfer mechanisms. This leads to extensive experimental investigation on the natural convection of nanofluids. Different types of nanoparticles, such as aluminium oxide, copper oxide and silicon oxide, were mixed in a base fluid, and their heat transfer efficiency tested in natural convection. Moreover, no investigation on the natural convection of a ZnO-water nanofluid in a cavity has been reported.

1.3 Aim

This study aims to experimentally investigate the heat transfer efficiency of the natural convection of ZnO-water nanofluids in a differentially heated square enclosure from walls with almost uniform aspect ratio.

1.4 Objective

The objectives of this study were as follows:

- Obtain a stable ZnO-water nanofluid by using a two-step method with a surfactant
- Verify the stability of a ZnO-water nanofluid by measuring zeta potential and absorbency values
- Obtain viscosity of a ZnO-water nanofluid at different volume concentrations of 0, 0.09, 0.18, 0.36, 0.5 and 1 vol.% fraction at various temperatures

- Obtain the heat transfer coefficient at different volume concentration of 0, 0.09, 0.18, 0.36, 0.5 and 1 vol.% of a ZnO-water nanofluid at various temperature differences of hot and cold walls
- Obtain a Nusselt number (Nu) against a Rayleigh number (Ra) at different volume concentrations of 0, 0.09, 0.18, 0.36, 0.5 and 1 vol.% of a ZnO-water nanofluid

1.5 Scope of work

The ZnO-water nanofluids with different volume fractions of 0, 0.09, 0.18, 0.36, 0.5 and 1 vol.% are used to obtain a heat transfer coefficient at a temperature range between 10 and 33 °C. The Ra was varied between $7.9E+7$ and $8.9E+8$. The viscosity of the ZnO-water nanofluid was also measured experimentally with the same volume fraction at a temperature range between 10 and 60 °C.

1.6 Overview of dissertation

Chapter 2 presents a literature study of the formulation method and stability of the nanofluid, as well as a brief review on the thermal properties of nanofluids. Recent numerical and experimental studies of the natural convection of nanofluids in a differentially heated square enclosure are summarised. Chapter 3 explains the methodology of formulating the stable ZnO-water nanofluid. The experimental method is also demonstrated in detail. Chapter 4 compiles the experimental results of a ZnO-water nanofluid regarding its viscosity and heat transfer coefficient in natural convection. The results of the uncertainty are analysed. Chapter 5 shows the conclusion of the study.

2. Literature study

2.1 Introduction

In this chapter, the fundamental concepts of nanofluids, as well as their properties (thermal conductivity, viscosity, specific heat and density) are discussed. A summary of the recent numerical and experimental studies of the natural convection heat transfer of nanofluids in a differentially heated square enclosure has also been included in this chapter.

2.2 Formulation method for nanofluids

Nanoparticles do not simply mix and disperse in the base fluid. When the proper preparation method is not followed, the sedimentation and aggregation of nanoparticles will develop. Nanoparticles should be uniformly distributed in the base fluid with stable suspension. There are two ways of preparing the nanofluid: the one-step method and the two-step method [5].

2.2.1 One-step method

The one-step method is a process that produces nanoparticles through direct evaporation into a low-vapour pressure fluid. This method simultaneously produces and disperses the nanoparticles in the base fluid. Zhu, Lin and Yin [6] presented a new one-step method to prepare copper oxide (CuO)-ethylene glycol (EG) by the reducing chemical properties in EG under microwave irradiation. Then copper nanofluids are obtained without any agglomeration. The one-step method offers better stability, but is much more expensive on an industrial scale.

2.2.2 Two-step method

The two-step method is a common technique for preparing nanofluids [7–9]. Nanoparticles and base fluids should be prepared separately and then mixed together with a magnetic stirrer,

ultrasonic bath, ultrasonicator or a high-pressure homogeniser.

2.2.3 Surfactant

For chemical stability, a surfactant (dispersant), such as ammonium hydroxide, sodium hydroxide, hydrazine hydrate and sodium borohydrate, is added to the nanofluid [5]. Hwang, Lee, Lee, Jung, Cheong, Lee, Ku and Jang [10] found that the stability of the nanofluid depends on the suspended nanoparticles and its base fluid. The UV-vis spectrum analysis method is used to estimate the nanofluid's stability. The addition of sodium dodecyl sulphate (SDS) improves the stability of the nanofluid because the SDS increases the zeta potential (surface charge) of nanoparticles and creates the repulsion force between them. Wang, Zhu and Yang [11] added the sodium dodecylbenzene sulfonate (SDBS) to a aluminium oxide (Al_2O_3) and CuO-water nanofluid to enhance the stability of the nanofluid. They found that the SDBS helped the dispersion of nanoparticles in the base fluid. This also helped increase its thermal conductivity. Yang, Du, Zhang and Cheng [12] found the optimum stability of Al_2O_3 -water nanofluid by adding a 0.3% mass fraction of polyacrylic acid (PAA) and cetyl trimethyl ammonium bromide (CTAB). Anandan and Rajan [13] mixed CTAB with CuO-nanofluid by using ultrasonication. It was visually observed that CTAB enhances the stability of the nanofluid. Chopkar, Das, Manna and Das [14] added 1 vol.% of tetramethylammonium hydroxide (TMAH) into the nanofluid for better dispersion. The heat transfer characteristics improved with a low volume concentration of the TMAH surfactant in a pool boiling heat transfer. The lauric acid surfactant is commonly used in magnetic nanofluid for steric stabilisation purpose [15, 16] No heat transfer effect is found in lauric acid.

Table 1: Surfactants used for nanofluid stability

Surfactant	Authors	Nanofluid	Effect
SDS	Hwang et al. [10]	Various nanofluids [Multi-walled carbon nanotubes (MWCNT), fullerene, CuO, SiO ₂]	Improves stability for all nanofluids.
SDBS	Wang et al. [11]	Al ₂ O ₃ and Cu-water	Thermal conductivity increases with the increment in surfactant,
PAA CTAB	Yang et al. [12]	Al ₂ O ₃ -water	PAA is the most stable surfactant with 0.3% mass fraction of the nanoparticle.
CTAB	Anandan and Rajan [13]	CuO-water	Thermal conductivity increases when nanoparticles are well dispersed in the base fluid.
TMAH	Chopkar et al. [14]	Zirconium dioxide (ZrO ₂)	The addition of 1.0 vol.% of TMAH in a nanofluid gives better dispersion.

2.3 Stability of nanofluids

Stable suspension and good dispersion of nanoparticles are the most important requirements to formulate nanofluids. Nanoparticles have to disperse uniformly before they agglomerate each other. Once the agglomeration is formed in the nanofluid, the chemistry bonding is strong and it is hard to break down into primary nanoparticles [17]. The agglomeration and settlement of nanoparticles in the base fluid can cause a discrepancy in its thermal properties [18]. Therefore, stability of nanofluids is a crucial factor that impacts on the thermal properties for any applications. The stability evaluation methods for nanofluids will be discussed.

2.3.1 Zeta potentials analysis

Zeta potential is a physical property that exists in any particle suspension, material surface or macromolecule. Zeta potential can be used to optimise the formulation of suspensions [19]. It can also predict the stability of nanoparticles in the base fluid. The values of zeta potentials indicate the potential stability of the colloidal system [20]. The particles will repel each other when a high positive or negative zeta potential is found during suspension, so there will be less chance of the particles sticking to each other [10]. When the absolute value of zeta potential is higher than 30mV, the colloid is considered to be stable [19]. Zawrah, Khattab, Girgis, Daidamony and Abdel Aziza [21] measured the zeta potential to verify the stability of a Al_2O_3 -water nanofluid under different concentrations of SDBS as a surfactant. Kim, Bang and Onoe [22] found a large negative zeta potential in gold nanoparticle (Au-NP)-water, which indicates a stable characteristic of a nanofluid. Lee, Hwang, Jang, Lee, Kim, Choi and Choi [23] measured the zeta potential to verify the good dispersion of Al_2O_3 -DI water.

2.3.2 Spectral absorbency analysis

The spectrophotometer is an instrument that is employed to measure the amount of light that is absorbed by a medium. The intensity of light reaching a detector is measured by a passing beam of light through the sample. The stability of a nanofluid can also be checked by measuring its absorbency using a spectrophotometer [24]. The absorbency increases with an increase in the nanoparticle concentration, indicating a linear relationship between them [25]. The concentration of nanoparticles can be estimated by measuring the absorbency of nanofluids [26].

2.3.3 Sedimentation

The sedimentation of nanoparticles in the base fluid can be observed visually. If nanoparticles are not well mixed and distributed, particles tend to settle down, thus forming a thin layer of nanoparticles at the bottom. Zhu, Zhang, Tang, Wang, Ren and Yin [27] measured the weight of sedimentation nanoparticles for certain periods of time. The weight or volume of sedimentation that settles down during a certain period indicates the suspension stability of the nanoparticles in the base fluid. Photographs or video footage can be captured to observe the sedimentation for long periods.

2.4 General applications of nanofluids

Nanofluids open up new opportunities to develop nanotechnology-based thermal systems and medical applications, as well as an innovative engineering field. Recently, a large number of articles and review papers were published regarding potential applications of nanofluids. The applications of nanofluids can be split into four major fields, as indicated in Table 2.

Table 2 : Application of nanofluids and description of the field of potential application

Field of potential application	Description
Heat transfer applications	<ul style="list-style-type: none"> • Industrial cooling applications: The replacement of cooling and heating water with nanofluids has the potential to conserve great amounts of energy [28]. • Smart fluids: Control the flow of heat [29]. • Nuclear reactors: The water-cooled nuclear system has improved its performance and productivity by using nanofluids. More research has to be implemented [30].
Automotive applications	<ul style="list-style-type: none"> • Nanofluid coolant: A smaller size and better positioning of the radiator can be achieved by using nanofluids as coolants. It gives higher efficiency of heat transfer [31]. • Brake and other vehicular nanofluids: Brakes generate a considerable amount of heat due to friction. Brake oil is therefore affected by the heat generated by braking. Nanofluids can maximise performance in heat transfer [32].
Biomedical applications	<ul style="list-style-type: none"> • Nano-drug delivery: The integrated micro- or nano-drug delivery system can be used to monitor and control the target cell responses to understand biological cell activities or to enable drug development processes [33]. • Cancer therapeutics: Nanofluids are used in cancer imaging and drug delivery, taking advantage of the properties of nanofluids. A magnetic nanofluid is useful when guiding the particles up the blood stream with magnets to a tumour [33].

The use of nanofluids is not yet ready for industrial uses, as it is still in a research and development phase. Nevertheless, nanofluids show high potential in various areas.

2.5 Thermal conductivity

The small amount (usually less than 5% volume fraction) of guest nanoparticles in a base fluid is reported to increase the inherently poor thermal conductivity of the liquid [34, 35, 36]. The thermal transport phenomenon of nanofluids shows outstanding enhancement in thermal properties compared with a base fluid such as water, EG or oil. The low thermal conductivity of conventional fluids could be compensated for by adding nano-sized particles that have a significantly higher thermal conductivity.

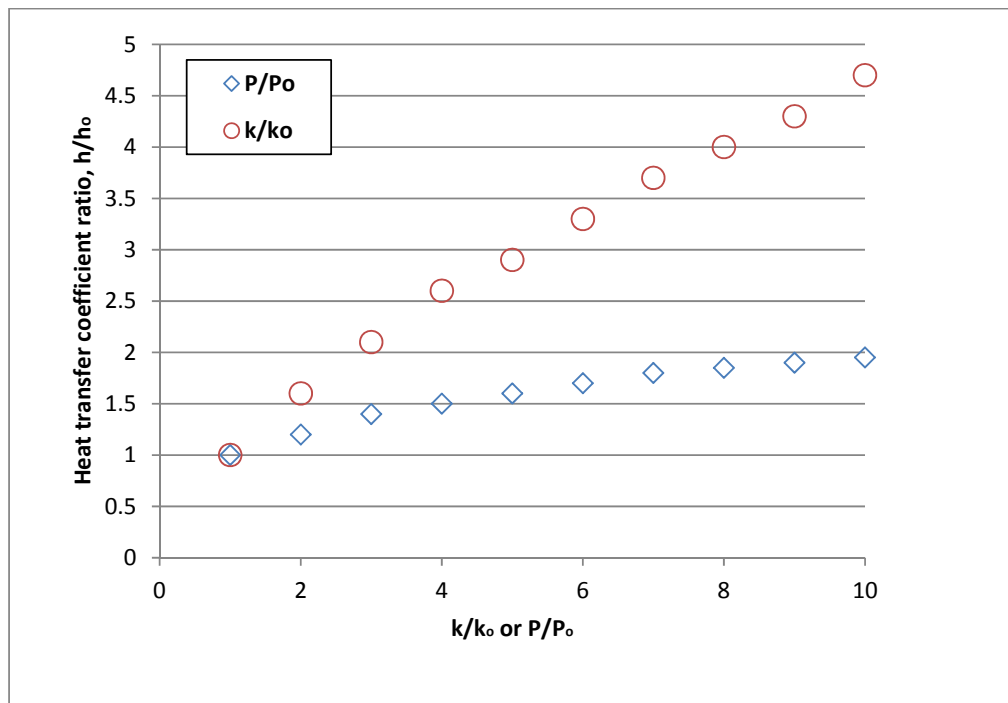


Figure 1: Effects of thermal conductivity and pumping power on heat transfer [1]

The initial work of Choi [1] reported that the convection heat transfer coefficients had more than doubled by adding nanofluids. The heat transfer coefficient ratio of nanofluids to base

fluids is directly proportional to the thermal conductivity ratio of nanofluids to base fluids, as shown in Figure 1. Eastman, Choi, Li, Yu and Thompson [37] reported a 40% increase in thermal conductivity by using copper nanofluids ($d_p < 10$ nm) in EG as a base fluid. Das, Putra, Thiesen and Roetzel [38] found a 35% improvement in thermal conductivity at 50 °C by suspending 4 vol.% of CuO ($d_p = 28$ nm) nanoparticles in water. Jana, Salehi-Khojin and Zhong [39] demonstrate that copper (Cu)-water nanofluids have a 74% increase in conductivity at 0.3 % volume fraction of the nanoparticles.

The traditional formulae of Maxwell's model [40], as shown in (Equation 1 and Bruggeman's model [41], as shown in Equation 2 were implemented to calculate the effective thermal conductivity of nanofluids as follows:

$$k_{nf} = k_{bf} \frac{k_{np} + 2k_{bp} + 2\varphi(k_{bf} - k_{np})}{k_{bf}(k_{np} + 2k_{bf} + \varphi(k_{bf} - k_{np}))} \quad (1)$$

$$k_{nf} = k_{bf} \frac{(3\varphi - 1)k_{np} / k_{bf} + [3(1 - \varphi) - 1] + \sqrt{\Delta}}{4}$$

$$\Delta = ((3\varphi - 1)k_{np} / k_{bf} + [3(1 - \varphi) - 1])^2 + 8 \frac{k_{np}}{k_{bf}} \quad (2)$$

Recently, the effective thermal conductive formulae were developed for nanofluids theoretically and experimentally [38, 42–45]. Most of the formulae are not only functions of thermal conductivity and volume fraction, but also depend on factors such as particle size, particle shape, temperature, base fluid behaviour and pressure. Sharifpur et al. [3] indicated that if the volume concentration of nanoparticles is less than 1 vol.%, the thermal conductivity of nanofluids can be predicted by most of the available models. They also found that most of the models, which are functions of particle size, could predict almost the same value under 1 vol.% concentration if the particle size is approximately 20 nm.

2.5.1 Thermal conductivity of ZnO-water nanofluids

Kim, Choi and Kim [42] reported that the thermal conductivity of a ZnO-water nanofluid at 1 vol.% concentration has been improved by 3.3%. Jeong, Li, Kwonb, Lee, Kim and Yun [43] found that the thermal conductivity of water as a base fluid at 1 vol.% concentration of ZnO increased by 4%. Colla, Marinelli, Fedele, Bobbo and Manca [46] experimentally measured the thermal conductivity of a ZnO-water nanofluid. They reported a 3.2% increase in thermal conductivity at 1 vol.% concentration in comparison to the base fluids. Jang and Choi [47] found that the thermal conductivity at 1 vol.% of a ZnO nanofluid improved by 5%. Yu, Xie, Lifei and Li [48] reported that the thermal conductivity of EG-based ZnO nanofluids at 1 vol.% concentration improved by 9%. Lee, Kim, Lee, Rhee, Kim and Kim [49] reported a 5% improvement in the thermal conductivity of ZnO-EG at 1 vol.% concentration. Table 3 shows the experimental results of the thermal conductivity of ZnO-water at 1 vol.% concentration.

Table 3: The thermal conductivity of a ZnO-water nanofluid

Author	Base fluid	Concentration	Size of particle (nm)	Enhancement of thermal conductivity
Kim et al. [42]	Water	1 vol.%	30 nm	3.3%
Jeong et al. [43]	Water	1 vol.%	20 to 40 nm	4%
Colla et al. [46]	Water	1 vol.%	60 nm	3.2%
Jang and Choi [47]	Water	1 vol.%	20 nm	5%
Yu et al. [48]	EG	1 vol.%	10 to 20 nm	9%
Lee et al. [49]	EG	1 vol.%	≤100 nm	5%

Thermal conductivity is not the only factor to influence the optimal performance of a nanofluid. Brownian motion, nano-convection, interfacial thermal resistance and the nanolayer also affect a nanofluid's heat transfer ability [50].

2.6 Viscosity of nanofluids

In convective heat transfer, the heat transfer coefficient relies on both the thermal conductivity and the viscosity of the heat transfer fluid. The particle concentration, temperature and particle size significantly influence nanofluid viscosity.

The theoretical formula of viscosity, which is based on the assumption of the linear relationship of viscous fluid containing a suspension of particles, is derived by Einstein's model [51], as shown in Equation 3.

$$\mu_{nf} = \mu_{bf}(1 + 2.5\varphi) \quad (3)$$

Brinkman's model [52], as shown in Equation 4, improves Einstein's model [51] to a nanoparticle concentration up to 4 vol.%.

$$\mu_{nf} = \frac{\mu_{bf}}{(1 - \varphi)^{2.5}} \quad (4)$$

Sunganthi and Rajan [53] reported an empirical formula for the viscosity of ZnO- water nanofluid for 0.25 vol.% to 2 vol.% (Equation 5).

$$\mu_{nf} = \mu_{bf} (1 + 11.97 \varphi) \quad (5)$$

Pak and Cho [54] observed that the viscosity of aluminium oxide (γ -Al₂O₃) and titanium dioxide (TiO₂) nanofluids with 10 vol.% concentration increased by 200 times and three times respectively, compared to the base fluids (water). Nguyen, Desgranges, Roy, Galanis, Maré, Boucher and Mintsa [55] found 210% enhancement of viscosity of Al₂O₃-water (36 nm) with 13 vol.% concentration. Bobbo, Fedele, Benetti, Colla, Fabrizio, Cesare and Barison [56] discovered a viscosity enhancement of 12.9 and 6.8% for 1 vol.% of single-walled carbon nanotubes (SWCNT)-water and TiO₂-water nanofluid respectively. Anoop, Sundararajan and Das [57] obtained 32% viscosity enhancement with 6 vol.% of CuO-EG nanofluid. Godson, Raja, Mohan Lala and Wongwises [58] observed an enhancement of 1.45 times in viscosity with 0.9 vol.% concentration of silver (AG)-water nanofluid.

A similar trend of viscosity enhancement with an increasing nanoparticle volume concentration has been proven in numerous published studies. The viscosity of base fluids increased significantly by adding a small amount of nanoparticles. However, there are no common empirical correlations or formulae available to estimate viscosity for all nanofluids. Experimental measurements of nanofluid viscosity are recommended for accurate results.

2.7 The specific heat, density and thermal expansion coefficient of nanofluid

Pak and Cho [54] used a mixture model of solid-liquid to express specific heat of the nanofluid as follows:

$$c_{p-nf} = (1 - \varphi)c_{p-bf} + c_{p-np} \quad (6)$$

The density and thermal expansion coefficient of the nanofluid are evaluated using the

average volume fraction ratio method, which is generally accepted by many researchers [59]. Pak and Cho [54] and Vajjha, Das and Mahagaonkar [60] experimentally confirmed good agreement between the experimental results and correlations. The density and thermal expansion coefficient of nanofluids are calculated as follows:

$$\rho_{nf} = (1 - \phi_{np})\rho_{bf} + \rho_{np}\phi_{np} \quad (7)$$

$$\beta_{nf} = \frac{(1 - \phi)\rho_{bf}}{\rho_{nf}} \beta_{bf} + \frac{\phi\rho_{np}}{\rho_{nf}} \beta_{np} \quad (8)$$

The thermophysical properties of the base fluid (water) and nanoparticles (ZnO) are summarised in Table 4.

Table 4: Thermophysical properties of water fluid and ZnO [61]

Property	Base fluid (water)	Nanoparticle (ZnO)
c_p (J/kg. K)	4 180	523
ρ (kg/m ³)	997.1 @ 25°C	5 606
k (W/mK)	0.607	25
μ (kg/ms)	8.91×10^{-4}	-
β (k ⁻¹)	2.1×10^{-4}	8.7×10^{-6}
α (m ² /s)	1.46×10^{-7}	0.583×10^{-7}

2.8 Natural convection of nanofluids

A natural convection cooling design could reduce the overall size of components, as well as pollution, noise and cost. However, natural convection inherently has a low heat transfer coefficient in comparison to other heat transfer methods. Many in-depth numerical studies and fewer experimental studies have been conducted on natural nanofluid convection. Table

5 summarises the recent numerical and experimental studies of natural nanofluid convection in a differentially heated square enclosure.

Khanafer, Vafai and Lightstone [62] numerically investigated natural convection heat transfer enhancement in a two-dimensional enclosure that utilises a Cu-water nanofluid. The model was proposed by Brinkman [52] and Wasp, Kenny and Gandhi [63] to determine the effective viscosity and thermal conductivity of nanofluids respectively. The heat transfer performance improved by 25% at a 0.2 vol.% concentration. Conversely, Putra, Roetzel and Das [64] observed a reduction in the heat transfer rate when nanoparticles were added to the base fluid. Hwang, Lee and Jang [65] theoretically investigated the natural convection of Al_2O_3 -water nanofluid to compare the results with the experimental data of Putra et al. [64]. The effective thermal conductivity is determined by the model of Jang and Choi [66] and the effective viscosity is calculated with various formulae. Heat transfer is enhanced as the nanoparticles become smaller or as the temperature and particle concentration increase.

Wen and Ding [67] experimentally studied a TiO_2 -water nanofluid. The mechanical shear mixing and electrostatic stabilisation techniques are used to formulate a stable nanofluid. The heat transfer coefficient of natural convection decreases when nanoparticle concentration increases. Ho, Chen and Li [68] numerically investigated this using various formulae for effective thermal conductivity and viscosity to identify the unclear behaviour of an Al_2O_3 nanofluid. They demonstrated that heat transfer performance depends on the adoption of various combinations of thermal conductivity and viscosity formulae, regardless of whether they deteriorate or improve. Oztopa and Abu-Nada [69] also numerically found that the heat transfer rate increases when the nanoparticle concentration increases. They showed that a low aspect ratio is more efficient in heat transfer than a high aspect ratio of the enclosure.

However, Santra, Sen and Chakraborty [70] reported that heat transfer deteriorates as the volume concentration of Cu nanoparticles increases. They numerically investigated this using the model of Garnett [71] and Bruggeman [41] with the semi-implicit method for pressure-linked equations – revised (SIMPLER) algorithm by assuming the nanofluid as a non-Newtonian fluid.

Öğüt [72] reported a noticeable improvement in heat transfer when the concentration of nanoparticles and the Ra increase. They used the models of Yu and Choi [44] and Brinkman [52] for the effective thermal conductivity and viscosity model respectively. The effects of varying the incline angle of enclosure were also investigated. The most efficient heat transfer rate occurred at an incline angle of 30° and deteriorated at 90° . After their theoretical investigation, Ho, Liu, Chang and Lin [73] experimentally investigated the natural convection heat transfer of an Al_2O_3 -water nanofluid. The nanofluid's thermophysical properties were experimentally measured as functions of temperature. The effective dynamic viscosity increased by 55% and effective thermal conductivity increased by 14% with the addition of 4 vol.% of Al_2O_3 nanoparticles. At lower concentrations of 1 vol.% with a high Ra ($\text{Ra} > 2 \times 10^7$), Ho et al. [73] observed an improvement in heat transfer performance, which deteriorated when the nanoparticle concentration was higher than 1 vol.%. This occurs because of the dominant characteristics of dynamic viscosity in the heat transfer coefficient model.

Alloui, Guiet, Vasseur and Reggio [74] used the Lattice Boltzmann method to perform a numerical simulation in a shallow rectangular enclosure. The heat transfer performance was led by viscosity, rather than thermal conductivity. At a lower Ra ($\text{Ra} < 10^3$), convective heat transfer improves significantly as nanoparticle concentration increases in the water.

Qi, He, Yan, Tian and Hu [75] used the two-phase Lattice Boltzmann method to investigate

the natural convection heat transfer. At a high Ra ($Ra = 10^5$), the Nu increases rapidly with increasing concentrations of Al_2O_3 -water nanoparticles.

Hu, He, Wang, Wang and Schlberg [76] numerically and experimentally investigated a TiO_2 -water nanofluid in a square enclosure. They found that natural convection heat transfer is more sensitive to an increase in viscosity than an increase in thermal conductivity. The heat transfer ability of a TiO_2 -water nanofluid is poorer than that of pure water at a low Ra. Ho, Chen, Yan and Mahian [77] also numerically and experimentally investigated natural convection in a cavity filled with an Al_2O_3 -water nanofluid. The top wall of the cavity is heated and the bottom wall is cooled. All the side walls are insulated. The Nu is increased by an increase in nanoparticle concentration. The results emphasise the importance of considering the sedimentation of nanofluids when using a numerical method. After experimental and numerical investigations, Hu, He, Qi, Jiang and Schlberg [78] reported an average increase of 2% in the Nu at a Ra of 6×10^7 at 0.25 vol.% concentration. However, when the nanoparticle concentration is increased to 0.77 vol.%, the Nu declines by an average of 4% in comparison to the base fluid.

Table 5: Previous research for the natural convection of nanofluid in a closed rectangular cavity

Author	Nanofluid and concentration	Particle size	Ra	Method	Heat transfer enhancement
Khanafer et al. [62]	Cu-water 0 to 20 vol.%	10 nm	10^3 to 10^6	Numerical	Improved
Putra et al. [64]	Al_2O_3 -water CuO-water 1 to 4 vol.%	131.2 nm 87 nm	10^6 to 10^8	Experimental	Deteriorated

Author	Nanofluid and concentration	Particle size	Ra	Method	Heat transfer enhancement
Hwang et al. [65]	Al ₂ O ₃ -water 0 to 5 vol.%	10 nm 15 nm 20 nm 50 nm	10 ⁶ to 10 ⁷	Numerical	Improved
Wen and Ding [67]	0 to 0.57 vol.%	Not specified	0.5 x 10 ⁴ –3.5 x 10 ⁴	Experimental	Deteriorated
Ho et al. [68]	Al ₂ O ₃ -water 0 to 4 vol.%	Not specified	10 ³ to 10 ⁶	Numerical	Improved and then deteriorated
Oztopa and Abu-Nada [69]	Cu-water Al ₂ O ₃ - water TiO ₂ -water 0 to 20 vol.%	Not specified	10 ³ to 5x10 ⁵	Numerical	Improved
Santra et al. [70]	Cu-water 0.05 to 5 vol.%	100 nm	10 ⁴ to 10 ⁷	Numerical	Deteriorated
Ögüt [72]	Cu-water CuO-water Al ₂ O ₃ - water Ag-water TiO ₂ -water 0 vol. % 8 vol. % 16 vol. % 20 vol. %	Not specified	10 ⁴ to 10 ⁶	Numerical	Improved and then deteriorated

Author	Nanofluid and concentration	Particle size	Ra	Method	Heat transfer enhancement
Ho et al. [73]	Al ₂ O ₃ - water 0.1 to 4 vol.%	33 nm	6.21 x 10 ⁵ to 10 ⁸	Experimental	Improved and then deteriorated
Alloui et al. [74]	Cu-water Al ₂ O ₃ -water TiO ₂ 0 to 20 vol.%	Not specified	10 ⁰ to 10 ⁸	Numerical	Improved
Qi et al. [75]	Al ₂ O ₃ -water 0 to 5 vol.%	Not specified	10 ³ to 10 ⁵	Numerical	Improved
Hu et al. [76]	TiO ₂ -water 3.85 wt% 7.41 wt% 10.71 wt%	10 nm	4 x 10 ⁴ to 2.4 x 10 ⁸	Experimental and numerical	Improved
Ho et al. [77]	Al ₂ O ₃ -water 0 to 4 vol.%	33 nm	6.21 x 10 ⁵ to 2.56 x 10 ⁸	Experimental and numerical	Improved
Hu et al. [78]	Al ₂ O ₃ - water 0 to 3 wt%	30 nm	3.0 x10 ⁷ to 7x10 ⁷	Experimental and numerical	Improved and then deteriorated

Inconsistent results of numerical and experimental investigations of the natural convection of nanofluids, as well as a lack of knowledge on this matter, encourage better experimental investigation of the heat transfer characteristics of nanofluids.

2.9 Summary and conclusion

The nanofluids' thermal properties and heat transfer potential were investigated in this chapter. Many factors need to be considered to determine empirical formulae for the thermal

properties of nanofluids, such as the nanoparticle volume concentration, stability and dispersion of the nanofluid, type of base fluid, temperature, and nanoparticle type, size and shape. However, recent studies were unable to accurately predict the thermal properties of nanofluids to estimate the heat transfer efficiency of nanofluids. Additionally, most of the experimental data did not correspond with previous studies under the same conditions. A more precise systematic experiment is required to understand the fundamental physics of energy transport in nanofluids. Theoretical predictions should be made in terms of the agreement with experiments regarding concentration, particle size and temperature dependence.

The natural convection heat transfer of nanofluid is difficult to predict numerically, as demonstrated in Table 5, which shows inconsistent results. More experimental studies are encouraged to measure the heat transfer coefficient in natural convection. Recent studies found the optimistic thermal conductivity enhancement in ZnO nanofluid [79, 53], but the heat transfer natural convection of ZnO-water nanofluid has not been reported yet.

3. Method

3.1 Introduction

The purpose of this chapter is to demonstrate an experimental setup that was used to conduct natural convection heat transfer in the cavity. The methodology of formulating the stable ZnO-water nanofluid is presented, and the procedure of the experiment is explained.

3.2 Nanofluids

3.2.1 Formulating nanofluids

The nanoparticles should be well dispersed in the base fluid to form a homogeneous colloid. ZnO nanoparticles with an average size of 20 nm, which were obtained from Nanostructured & Amorphous Materials Inc. in the USA, and de-ionised water, which was obtained from Merck in South Africa, were used to prepare the nanofluid. To verify manufacturer information, transmission electron microscopy (TEM) images were taken (see Figure 2a). A dry ZnO powder depicts an aggregation of particles that needs to be broken down (see Figure 2b).

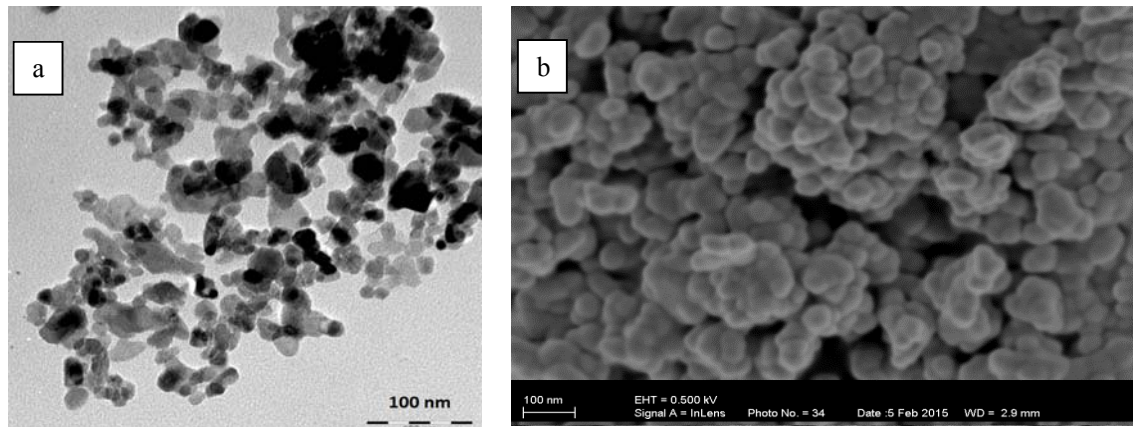


Figure 2: TEM image of ZnO-water nanofluid (a); and scanning electron microscopy (SEM) image of a dry powder of ZnO particles (b)

The nanofluids were prepared using a two-step method, and different surfactants were examined. Finally, tetramethylammonium hydroxide pentahydrate (TAHP), which was obtained from Sigma-Aldrich in the USA, was found to formulate a stable colloid. The amount of the surfactant that was added to the nanofluid was 1 vol.% of the nanoparticles. Ultrasonic energy was then applied using an ultrasonicator (Q-700, Qsonica) with 20 KHz and 700 W to disperse and break down the aggregation of nanoparticles. Sharifpur, Ghodsinezhad, Meyer and Rolfes [80] illustrate that 3 kJ/ml of sonication energy density is sufficient to reduce the average aggregation size to the minimum for a ZnO-water nanofluid (see Figure 3).

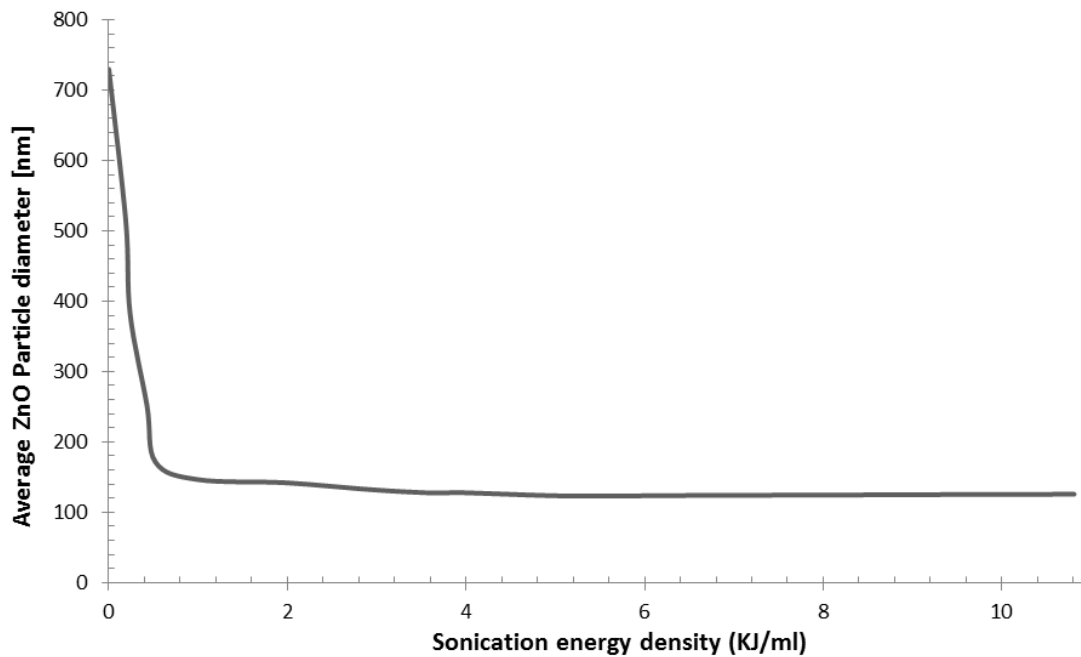


Figure 3: The effect of the sonication energy density of an average aggregation size on ZnO-water nanofluid [45]

3.2.2 Stability of nanofluid: zeta potential

The stability and suspension of nanofluids are verified by the zeta potential measurement using a Malvern Zetasizer Nano ZS (UK). Malvern Instruments [19] plotted zeta potential against pH to show stable and unstable zones, as shown in Figure 4. The problem with dispersion stability can be expected at pH values between 4 and 7.5 when absolute zeta potential is below 30 mV.

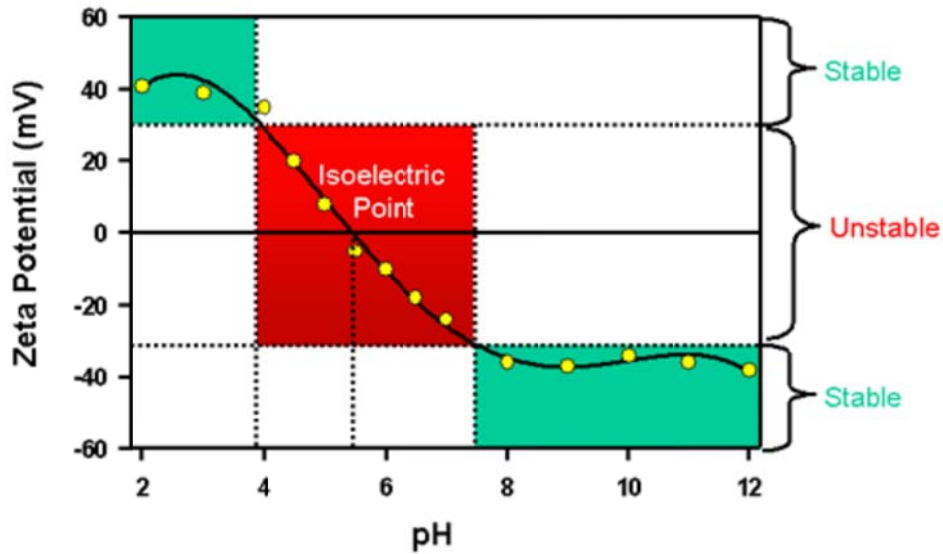


Figure 4: A stability plot of zeta potential versus pH [19]

Absolute zeta potential and pH value at different concentrations of ZnO nanofluid are measured as shown in Table 6. All concentrations show more than an absolute value of 30 mV at a pH value greater than 9. The colloids with zeta potentials greater than an absolute of 30 mV are considered as stable solutions at a pH greater than 7.5. [23].

Table 6: The effect of different concentrations on zeta potential of ZnO-water nanofluids

Concentration (ϕ)	ZP (mV) (absolute value)	pH
0.033 wt% (0.006 vol.%)	34	9
0.33 wt% (0.06 vol.%)	42	10.3
0.672 wt% (0.12 vol.%)	47	10.55

The stability of a ZnO nanofluid with a 0.06 vol.% concentration is also examined at various temperatures by measuring the zeta potential value as shown in Figure 5. As the temperature of a ZnO nanofluid increases, the absolute value of the zeta potential is decreased. This

means that a ZnO nanofluid shows better stability at a low temperature.

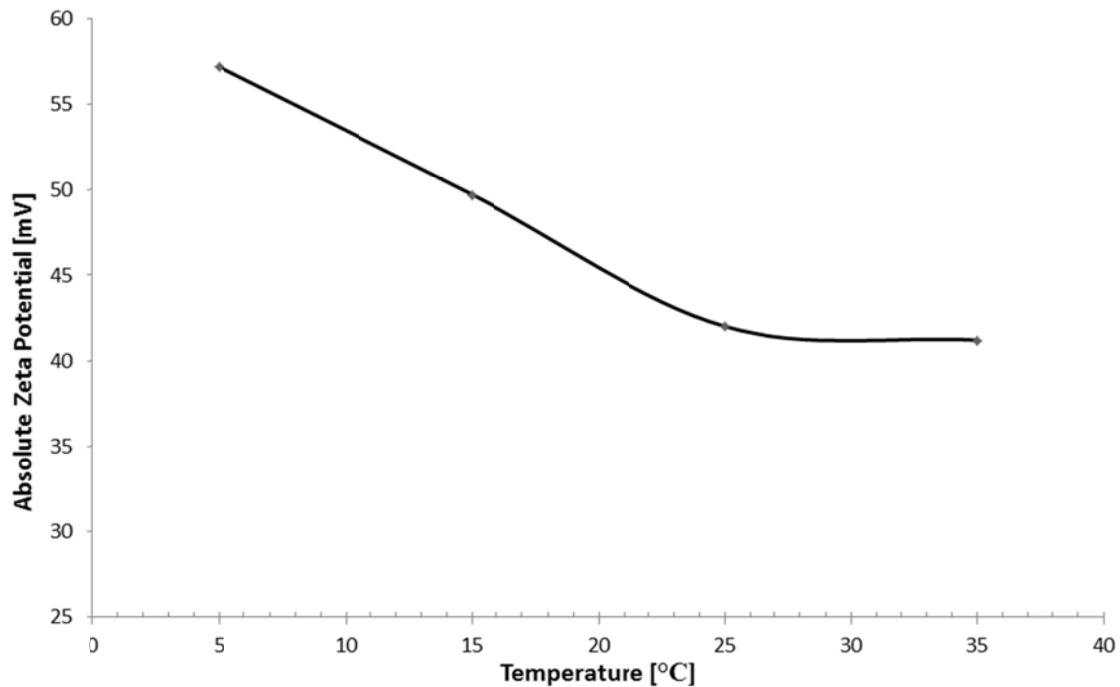


Figure 5: The influence of temperature on the zeta potential value of a ZnO-water nanofluid with a 0.06 vol.% concentration

3.2.3 Stability of nanofluid: spectrophotometer

The nanofluid stability is also examined using a spectrophotometer (Jenway 7315) with an accuracy of ± 2 nm for wavelength and a standard deviation of ± 0.01 absorbance at 1.0 absorbance. This method can estimate the colloidal concentration at a certain time as the sedimentation of nanoparticles increases [81]. The peak absorbance of 2.293 with the sample of 0.0018 vol.% of ZnO-water nanofluid occurs at a wavelength of 230 nm as shown in Figure 6.

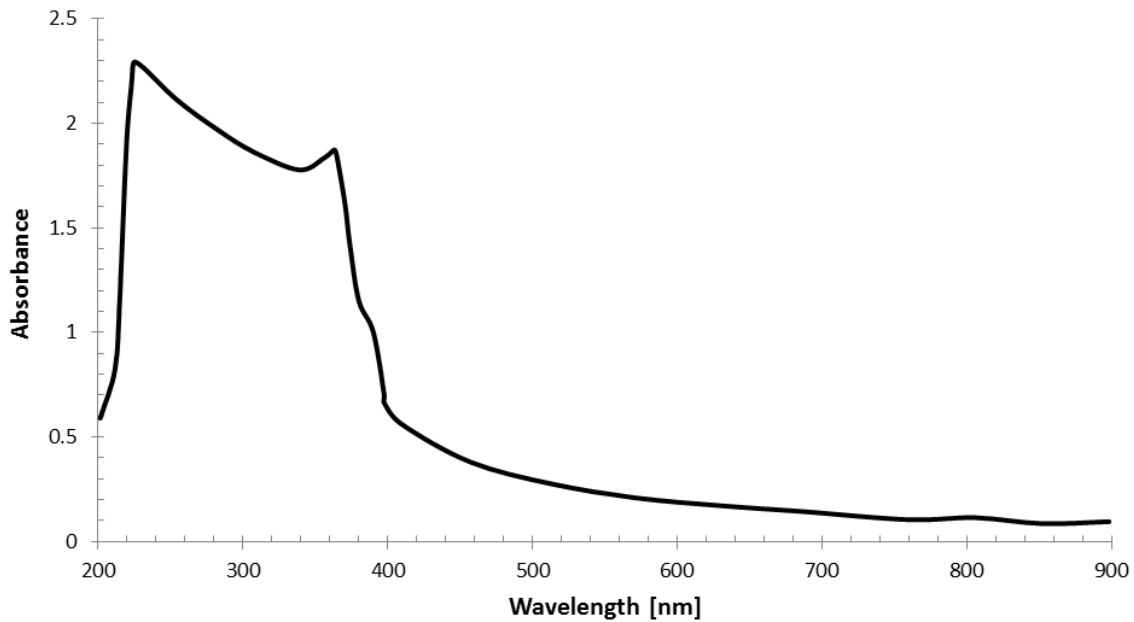


Figure 6: Absorbance of 0.0018 vol.% ZnO-water nanofluid versus wavelength

The absorbance of a nanofluid varies with the changing concentration of the sample due to the sedimentation of nanoparticles in the base fluids. The normalised concentration indicates that the concentration percentages changed from the initial concentration of the nanofluid, which was obtained over nine hours as shown in Figure 7. This indicates that no sedimentation occurred during the experiment period.

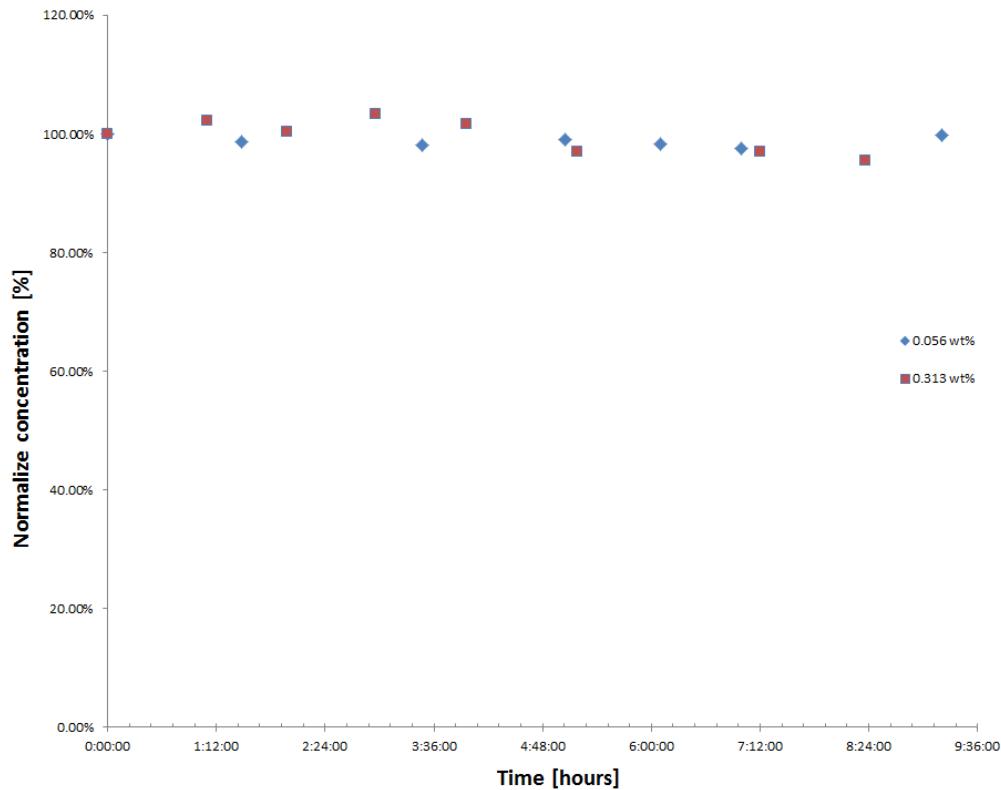


Figure 7: The effect of time on the concentration of ZnO-water

3.3 Experiment method

3.3.1 Heat exchanger and cavity design

A novel counter flow shell and tube heat exchanger, with the same hydraulic diameter (10.7 mm), has been designed and manufactured with a copper tube to serve as a heat source and a heat sink. Shell and tube exchangers consist of baffles that are placed between the tubes in order to force the shell side fluid to flow across the shell so that it enhances heat transfer to produce an almost constant temperature wall. Two heat exchangers are built and attached to the sides of the cavity, which are the experimental test sections. The constant temperature thermal baths are connected to each heat exchanger and circulate hot and cold water through respective heat exchangers.

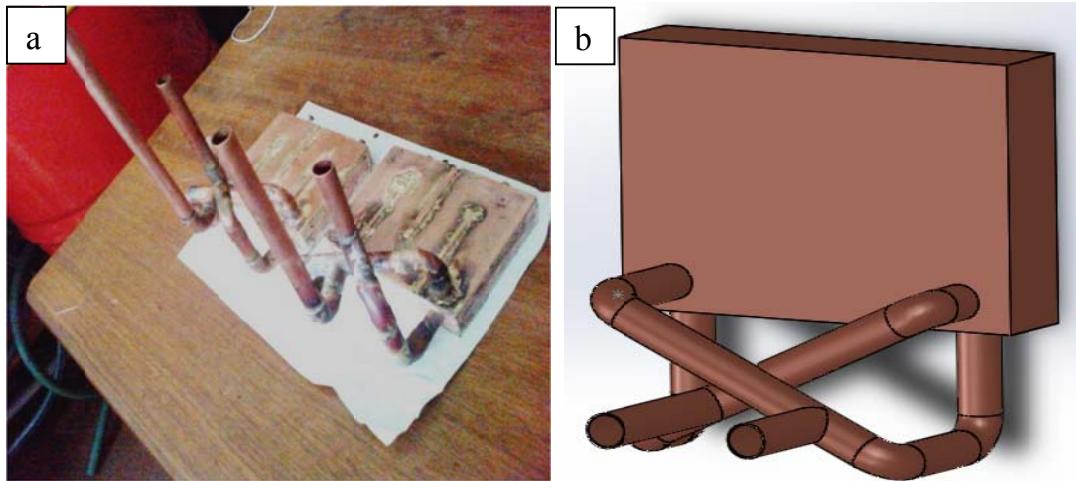


Figure 8: Heat exchanger (a) and solid work design of heat exchanger (b)

The rectangular cavity has two differently heated vertical walls (heat exchangers) at opposite sides with a height and width of 96 mm and 120 mm respectively. The distance between the two walls, as characteristic length, is 102 mm. The rest of the cavity is built with polycarbonate with a thermal conductivity of 0.19 W/m.K to 0.22 W/m.K at 23 °C [82]. Detail dimensional drawings and a bill of material for the cavity (test section) are demonstrated in Appendix A.

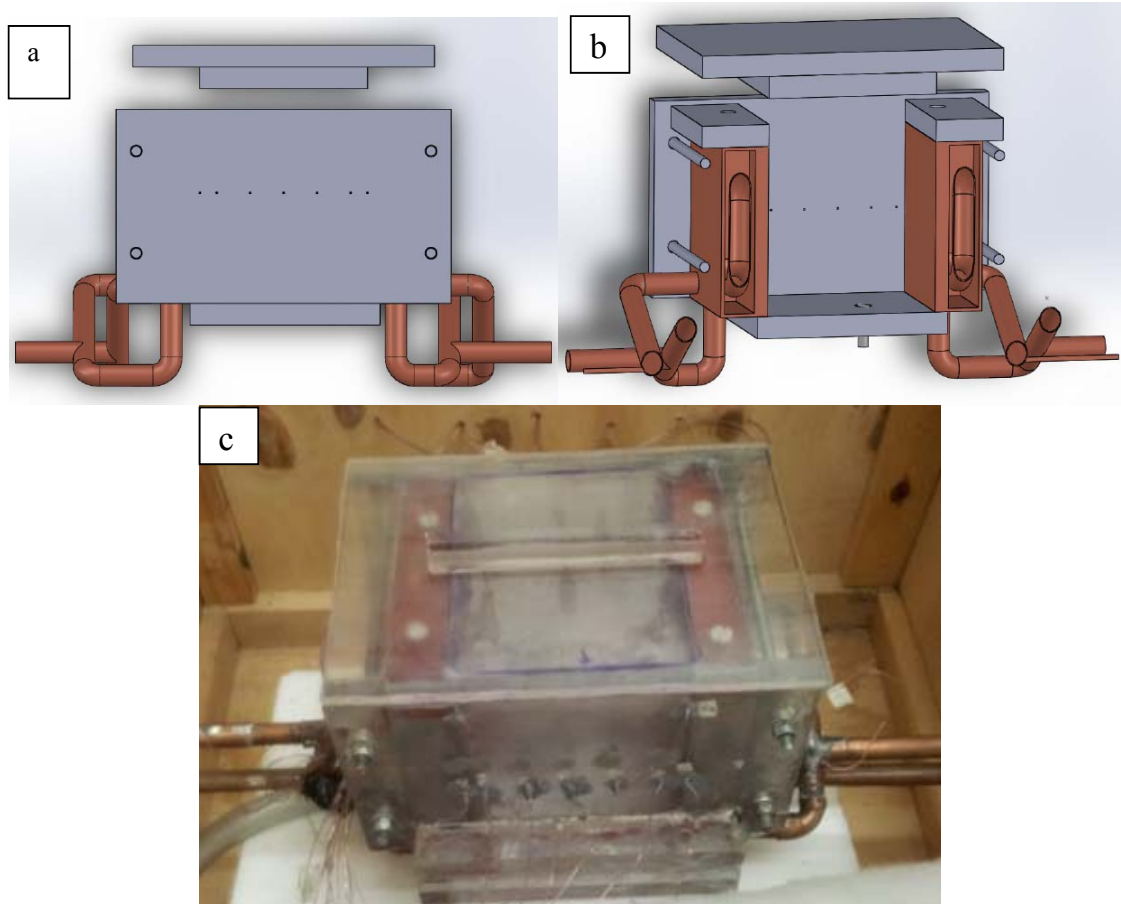


Figure 9: Cavity design by solid work (a), its section view (b) and the actual cavity (c)

3.3.2 Test section

In the test section, 27 thermocouples are installed as shown in Figure 10. The channels 1 and 2 measure the hot water inlet and channels 3 and 4 measure the hot water outlet from the heat exchanger. Channels 16 and 17 measure the cold water inlet and channels 18 and 19 measures the cold water outlet from the cold wall heat exchanger. Two thermocouples are connected at each inlet and outlet to achieve accurate results. The temperature differences at the inlet and outlet of the heat exchanger will indicate heat transfer between the heat exchanger and the test medium in the cavity. The distance between the thermocouples in the

test section (channels 6, 7, 8, 9, 10, 11, 12, 13 and 14) is 10 mm equally distributed except for channels 6 and 14, which are placed 5 mm closer to the wall. At the centre of the test section, four thermocouples (channels 24, 25, 26 and 27) are placed vertically to demonstrate temperature differences at the top and bottom of the test mediums. Three thermocouples are installed at the hot wall (channels 5, 20 and 21) and at the cold wall (channels 15, 22 and 23) respectively to ensure temperature distribution in the heat exchanger.

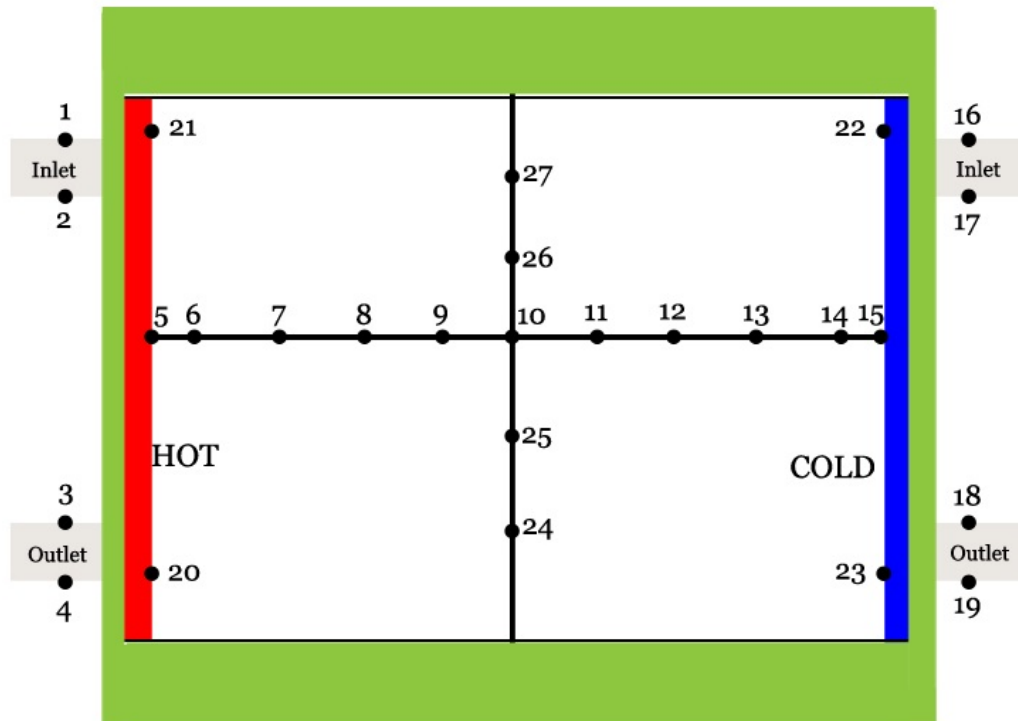


Figure 10: Sketch of the experiment test section and thermocouple location

Table 7: Thermocouple location

Thermocouple channel number	Thermocouple location
1,2	Inlet of the hot wall heat exchanger
3,4	Outlet of the hot wall heat exchanger
5	On the hot wall in the test section
6	5 mm from the hot wall in the test section
7	20 mm from the hot wall in the test section
8	30 mm from the hot wall in the test section
9	40 mm from the hot wall in the test section
10	50 mm from the hot wall in the test section (centre of cavity)
11	40 mm from the cold wall in the test section
12	30 mm from the cold wall in the test section
13	20 from the cold wall in the test section
14	5 mm from the cold wall in the test section
15	On the cold wall in the test section
16, 17	Inlet of the cold wall heat exchanger
18, 19	Outlet of the cold wall heat exchanger
20	On the hot wall at the top in the test section
21	On the hot wall at the bottom test section
22	On the cold wall at the top in the test section
23	On the cold wall at the bottom test section
24	4.5 mm from the bottom at the centre of the test section
25	25 mm from the bottom at the centre of the test section
26	71 mm from the bottom at the centre of the test section
27	92 mm from the bottom at the centre of the test section

3.3.3 Experimental setup and procedure

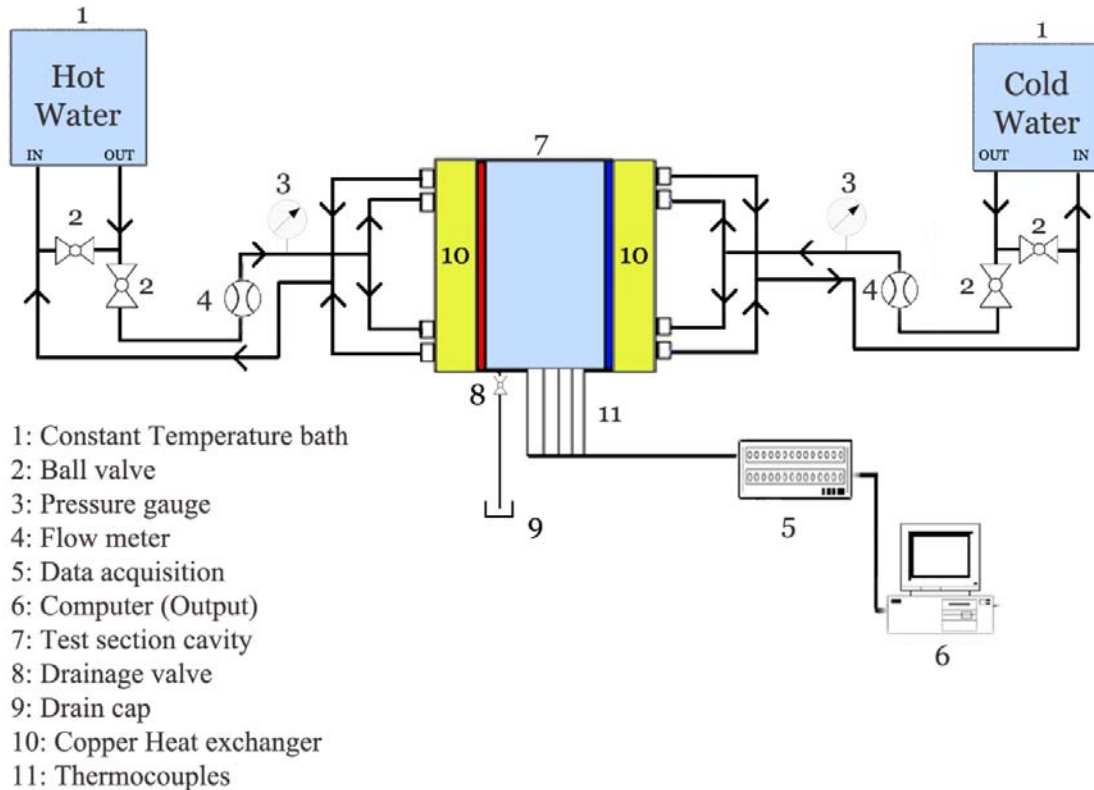


Figure 11: A schematic diagram of the experimental setup

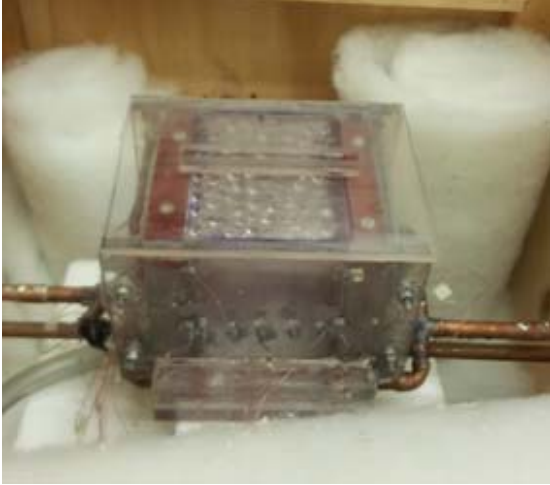



Figure 11 shows the simplified schematic diagram of the experimental setup for testing the natural convection of nanofluids. The rectangular cavity has two differentially heated vertical walls at opposite sides with heights and widths of 96 mm and 120 mm respectively. The distance between the two walls, as a characteristic length, is 102 mm. A novel counter flow shell and tube heat exchanger, with the same hydraulic diameter of 10.7 mm, have been designed and manufactured with copper to serve as a heat source and a heat sink. The rest of the cavity was built with polycarbonate, which has a thermal conductivity of 0.19 to 0.22 W/m.K at 23 °C [83]. To minimise ambient heat loss, the test cell is covered with a big wooden box, and gaps are filled with insulation polystyrene material (insulation = 20 cm with

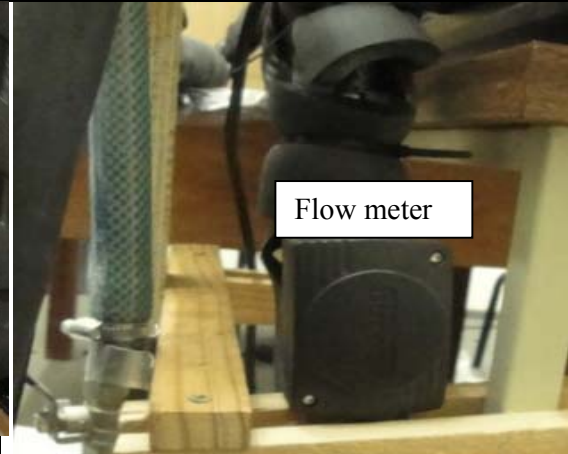
$k = 0.034 \text{ W/m.K}$).

Two constant Polyscience PR20R-30 (USA) thermal baths with accuracies of $0.005 \text{ }^\circ\text{C}$ are separately connected to each heat exchanger. These thermal baths supply a constant heat source and heat sink for the hot and cold walls respectively. The heat exchangers' performance is examined in an air-filled cavity, which results in a deviation of $0.5 \text{ }^\circ\text{C}$ at various spots on the surface of the heat exchangers.

Two Burkert 8081 ultrasonic flow meters (Germany) with $\pm 2\%$ accuracy are installed to measure the flow rate of the water that circulates from the constant thermal bath to the heat exchangers. The temperature is measured with Type-T Omega Engineering thermocouples (USA), with the part number TT-T-30-SLE (ROHS). These thermocouples have an accuracy of $0.02 \text{ }^\circ\text{C}$ after calibration. Temperature and flow rates are collected by data acquisition using SCXI-1303, an isothermal terminal block from National Instruments (USA), which uses LabVIEW software. For each set of experiments, 8 200 samples are measured at a frequency of 2 Hz. After 60 minutes, the temperature of the nanofluid inside the cavity is stabilised with a deviation of less than 0.1%. Therefore, the last 1 000 samples are used for the results. The experimental procedure is described with the images as shown in Table 8.

Table 8: Experiment procedure

	
<p>1. The test cavity is fully insulated with cotton wool, insulating a sponge piece and wooden box. Thermocouples are installed in the test section.</p>	
	
<p>2. The thermocouples from the test sections are connected to the data acquisition (National Instrument, SCXI-1303)</p>	



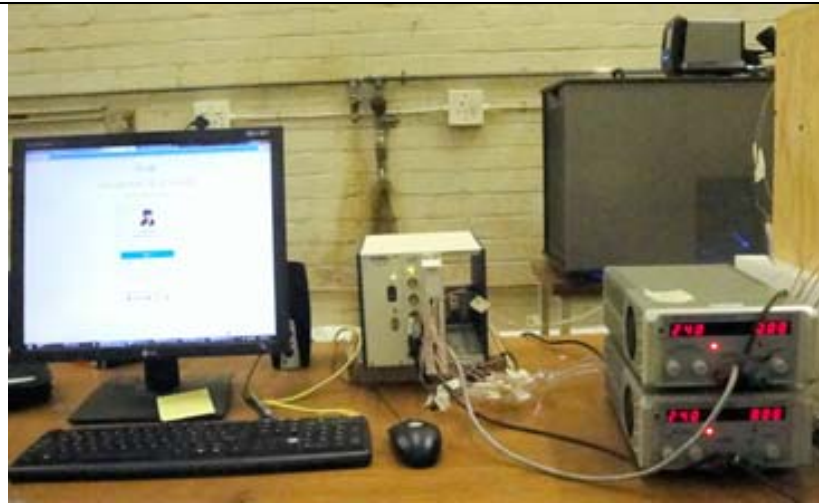
3. Pressure and ultrasonic flow meters are connected to a computer to record measurements during the experiment.



4. The thermal baths provide water of a constant temperature to the heat exchangers. The pump power and temperature can be adjusted by the thermal bath.



5. The nanofluid is poured into the cavity. The cavity is then closed with a lid and insulation cover.



6. When it has reached the steady-state condition in the test section, all the data must be measured and saved on the computer.

3.4 Physical configuration and formula

Figure 12 shows the two-dimensional physical configuration with the relevant notation and boundary condition for the natural convection of a nanofluid in a cavity. In this configuration, g is the gravitational acceleration, T_H is the temperature of the hot wall, T_C is the temperature of the cold wall, L_c is the characteristic length of the geometry, and H is the height of the cavity. Adiabatic conditions are assumed on the horizontal boundaries. Heat transfer occurs through the enclosure due to the different surface temperatures at the vertical walls.

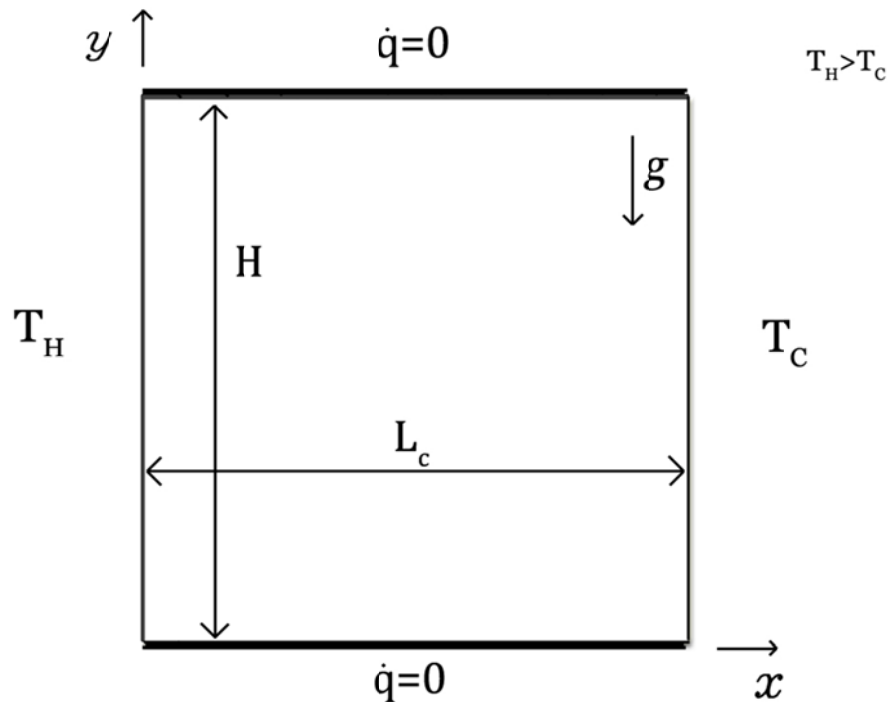


Figure 12: A schematic representation of a cavity problem for the natural convection flow, together with the relevant notation and boundary condition

The heat transfer rate of hot heat exchangers is calculated as follows:

$$\dot{Q}_{hot} = \dot{m}_{hot} c_p (T_{in} - T_{out}), \quad (9)$$

where T_{in} and T_{out} are the temperatures at the inlet and outlet of the heat exchanger

respectively. A deviation of less than 5% was found in the heat balance between the heat source and the heat sink, which indicates that a small amount of heat leaked into the atmosphere. The heat transfer by radiation between the hot and the cold walls is assumed to be negligible. The heat transfer coefficient of the nanofluid is calculated as follows:

$$\bar{h}_{nf} = \frac{\dot{Q}}{A(T_H - T_C)} \quad (10)$$

A is the surface area of the heated wall. The dimensionless Nu is calculated using the heat transfer coefficient (see Equation 6), which represents the ratio of convective heat transfer to conductive heat transfer.

$$Nu_{nf} = \frac{\bar{h}_{nf} L_C}{k_{nf}} \quad (11)$$

In the equation, k_{nf} is the effective thermal conductivity of the nanofluid. The model of Wasp et al[63] was used in the calculation. The dimensionless Ra is calculated as follows:

$$Ra_{nf} = \frac{g\beta_{nf}\rho_{nf}^2 L_C^3 (T_H - T_C)}{\mu_{nf} k_{nf}} \quad (12)$$

The viscosity of the nanofluid is experimentally measured with different nanoparticle concentrations between 10 and 60 °C by using an SV_10 viscometer of A&D Instruments (Japan), which has an accuracy of $\pm 3\%$ and repeatability of 1%. The thermophysical properties are calculated based on the average temperatures of the hot and cold walls respectively as follows:

$$T_{ave} = \frac{(T_H + T_C)}{2} \quad (13)$$

3.5 Summary and conclusion

The method of formulating ZnO-water nanofluid is demonstrated. The stability of ZnO-water nanofluid is validated to use for more than nine hours without any settlement. The experimental setup and procedures are described in this chapter. The rectangular test section consists of a height and width of 96 mm and 120 mm respectively, and the distance between the hot and cold walls is 102 mm. The Ra is varied between $9E+7$ and $9.8E+8$. All boundary condition of the test sections are defined by a constant temperature from two side walls that face each other. The other side of the test section is insulated to minimise heat loss. The methodology of calculating the heat transfer coefficient, average Nu and Ra are presented.

4. Result

4.1 Introduction

In this chapter, the heat transfer coefficient of ZnO-water nanofluid is evaluated at different volume fractions at the temperature range between 10 and 33 °C. The viscosity of ZnO-water nanofluid is experimentally measured to gain accurate results. Dimensionless Ra and Nu are calculated to compare the effect of ZnO-water nanofluid against pure water in a natural convection heat transfer.

4.2 Non-dimensional temperature versus non-dimensional distance

Non-dimensional horizontal temperature distribution inside the cavity is plotted against the non-dimensional distance of the cavity as shown in Figure 13.

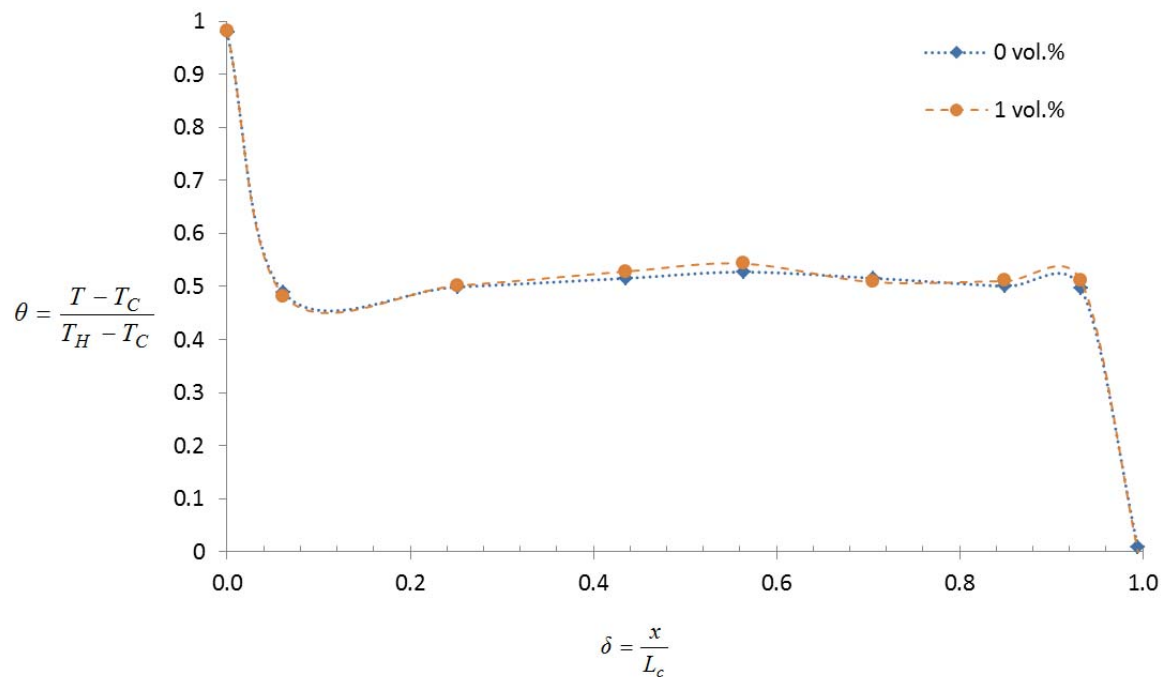


Figure 13: The non-dimensional temperature versus the non-dimensional distance in the cavity

The temperatures observed at the midpoint are slightly higher than the mean value of the hot and cold walls due to the higher thermal conductivity of the nanofluid.

4.3 Effect of volume fraction and temperature on the viscosity of ZnO-water nanofluids

The experimental measurement of the viscosity of ZnO-water nanofluid is shown in Figure 14. The viscosity of five samples of ZnO-water nanofluid at a volume fraction from 0 to 1 vol.% are investigated at temperatures ranging between 10 and 60 °C. As expected, the viscosity of the nanofluid increases with an increase in nanoparticle concentration. For example, the viscosity of nanofluid at 1 vol.% is 24% higher than the viscosity of the base fluid at 20 °C. The nanofluid viscosity decreases when the temperature increases. Moreover, at a high temperature, a deviation of the viscosity of different volume fractions is smaller in comparison to the low temperature.

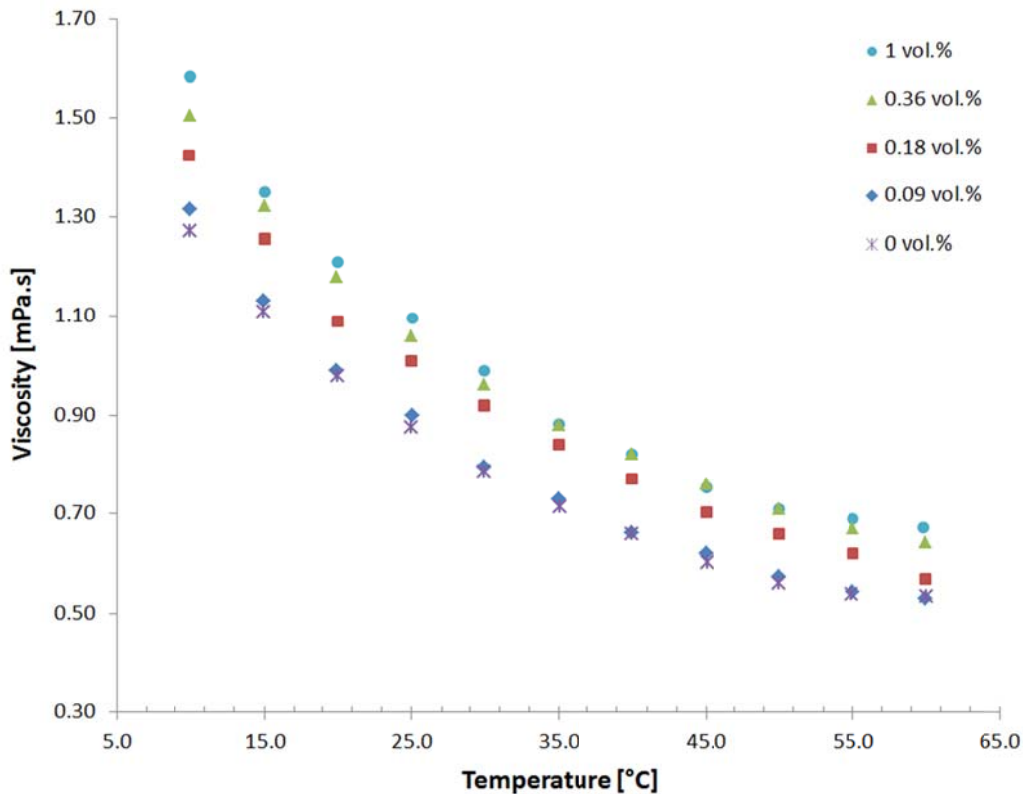


Figure 14: The effect of volume fraction and temperature on the viscosity of ZnO-water nanofluid

The Einstein viscosity model [51] (see Equation 3) predicts 20% less than the experimental measurement of viscosity at a temperature of 20 °C for 1 vol.%. At a low concentration, Brinkman's model [52] (see Equation 4) predicts approximately the same value as Einstein's model. Sunganthi and Rajan [53] (see Equation 5) reported an empirical formula for the viscosity of a ZnO-water nanofluid between 0.25 and 2 vol.%. The experimental result of the 1 vol.% concentration of a ZnO nanofluid shows higher viscosity than the theoretical value as shown in Figure 15.

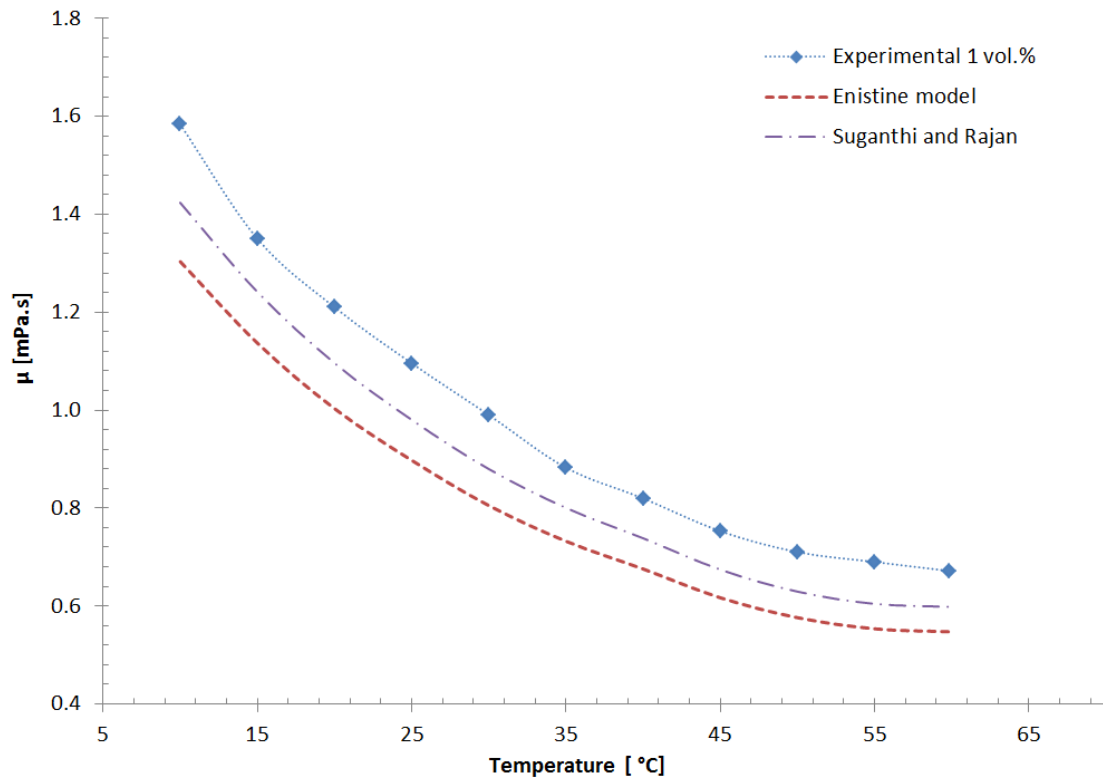


Figure 15: The viscosity of a ZnO nanofluid with theoretical and experimental measurements

4.4 Heat transfer coefficient for different mass fractions of ZnO-water nanofluid

The experimental study of the natural convection of a ZnO-water nanofluid for the volume fractions 0, 0.09, 0.18, 0.36, 0.5 and 1 vol.% and Ra between E+7 and 9.8E+8 are performed in a differentially heated cavity. The average natural convection heat transfer coefficient is measured with the different volume fractions of ZnO nanofluid at various temperatures ranging between 10 and 32 °C, as shown in Figure 16.

The natural convection heat transfer coefficient deteriorates by an average of 12% in comparison to the base fluid. Initially, the natural convection heat transfer coefficient is significantly reduced by adding ZnO nanoparticles to the base fluid. Subsequently, it fluctuates, but gradually decreases as the volume fraction of a ZnO nanofluid increases. The result does not show any optimum volume fraction that enhances the natural convection heat transfer coefficient of a ZnO nanofluid. To the contrary, Ho et al. [73] and Wen and Ding [67] used Al₂O₃ and TiO₂ nanoparticles respectively in the base fluids and reported the optimum increase of heat transfer coefficient at 0.1 and 1.2 vol.% respectively.

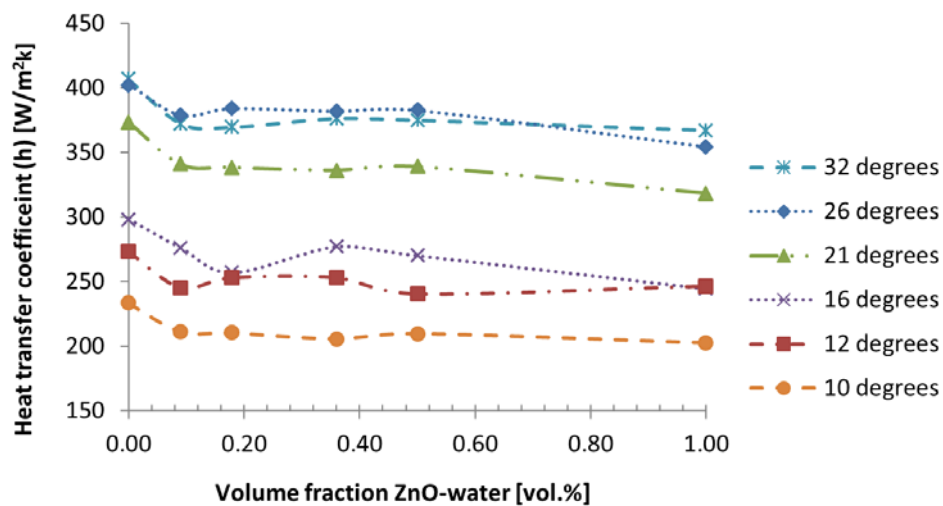


Figure 16 : The heat transfer coefficient for the different volume fractions of a ZnO

nanofluid at various temperature differences between the hot and cold walls

4.5 The effect of changing ZnO-water nanofluids' Ra on Nu with different mass fraction

The average Nu and Ra were alternately changed at different nanoparticle concentrations as shown in Figure 17. As expected, the average Nu increases as the Ra increases, but the average Nu decreases as the volume fraction of the nanofluid increases. Therefore, adding ZnO nanoparticles to water deteriorates the average Nu of the nanofluid. The average Nu's deterioration is more pronounced at a low Ra. All raw data is summarised in Appendix C.

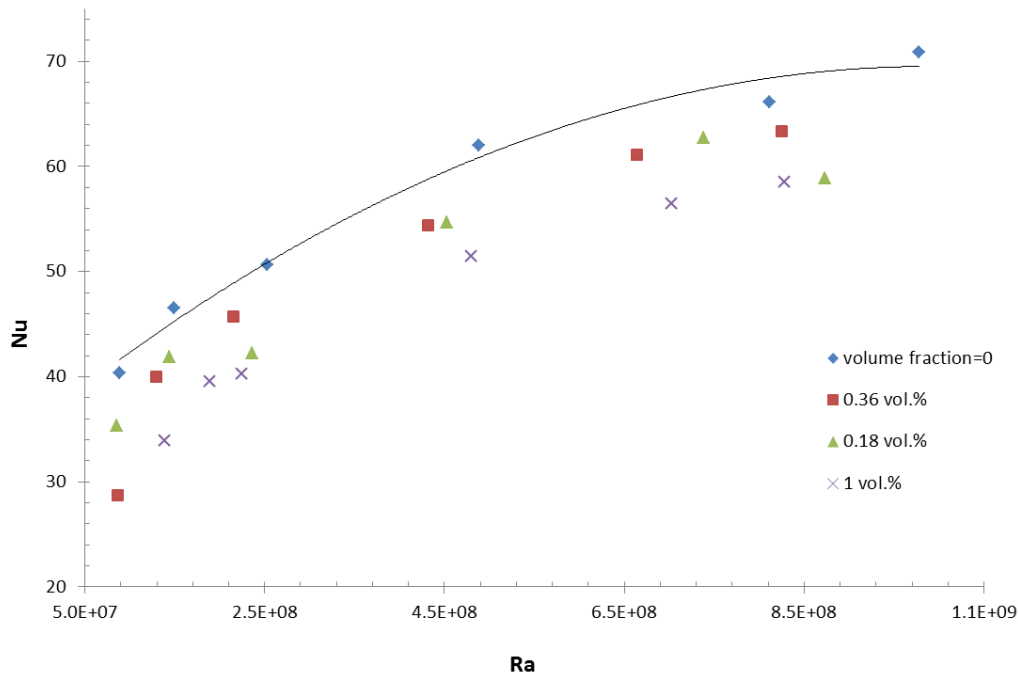


Figure 17 : The effect of a changing ZnO-water nanofluid's Ra on the Nu with a different volume fraction

4.6 Uncertainty analysis

The reliability of experimental results is examined by performing a relative uncertainty analysis [84]. The mean source of error could be the measurement of temperature, flow rate

and cavity size. Uncertainty of heat transfer (Q_{hot}), heat transfer coefficient (h) and Nu and Ra with a 1 vol.% concentration were found to be 2.93, 3.06, 3.05 and 4.36% respectively. The calculation is presented in Appendix D.

5. Conclusion

The experimental study of natural convection heat transfer in a rectangular cavity filled with a ZnO-water nanofluid at different volume fractions (0, 0.09, 0.18, 0.36, 0.5 and 1 vol.%) is examined at Ra between $7.9E+7$ and $9.8E+8$. The stability of a ZnO-water nanofluid is confirmed with a spectrophotometer and Malvern zetasizer. The absolute zeta potential value of a ZnO-water nanofluid with a 0.06 vol.% concentration at $5\text{ }^{\circ}\text{C}$ is measured at 57.2 mV, which indicates excellent stability. It is also found that a ZnO-water nanofluid showed better stability at a low temperature.

The experimental measurement of a viscosity of 1 vol.% ZnO-water nanofluid was reported as being 20% higher than the classical theoretical model, which is presented by the models of Einstein [51] and Brinkman [52]. The natural convection heat transfer in a rectangular cavity is investigated experimentally by adding a ZnO nanofluid for the first time. The results show that adding ZnO nanoparticles to a base fluid does not show an improvement in the natural convection heat transfer rate. The natural convection of nanofluids deteriorates when the nanoparticle concentration increases. The general effect of altering the thermophysical properties of a nanofluid does not benefit natural convection by applying a ZnO nanoparticle.

References

- [1] S. Choi, “Enhancing thermal conductivity of fluids with nanoparticles.,” *International Mechanical Engineering Congress Exposition*, p. 99–105, 1995.
- [2] S. Jana, A. Salehi-Khojin and W-H. Zhong, “Enhancement of fluid thermal conductivity by the addition of single and hybrid nano-additives,” *Thermochimica Acta*, vol. 462, no. 1–2, p. 45–55, 2007.
- [3] M. Sharifpur, T. Ntumba and J. Meyer, “Parametric analysis of effective thermal conductivity models for nanofluids,” *International Mechanical Engineering Congress and Exposition*, 2012.
- [4] M. Sharifpur, T. Ntumba and J. Meyer, “Parametric Analysis of Effective Viscosity models for Nanofluids,” *International Mechanical Engineering Congress and Exposition*, 2012.
- [5] L. Syam Sundar, K. Sharma, M. Naik and M. K. Singh, “Empirical and theoretical correlations on viscosity of nanofluids: a review,” *Renewable and Sustainable Energy Reviews*, vol. 25, pp. 670–686, 2013.
- [6] H-T. Zhu, Y-S. Lin and Y-S. Yin, “A novel one-step chemical method for preparation of copper nanofluids,” *Journal of Colloid and Interface Science*, vol. 277, no. 1, pp. 100–103, 2004.
- [7] C. Ho, J. Huang, P. Tsai and Y. Yang, “Preparation and properties of hybrid water-based suspension of Al_2O_3 nanoparticles and MEPCM particles as functional forced convection fluid,” *International Communications in Heat and Mass Transfer*, vol. 37, no. 5, pp. 490–494, 2010.
- [8] S. Suresh, K. Venkataraj, P. Selvakumar and M. Chandrasekar, “Synthesis of Al_2O_3 -Cu/water hybrid nanofluids using two step method and its thermo physical properties,” *Colloids and Surfaces A: Physicochemical and Engineering Aspects*, vol. 388, no. 1–3, pp. 41–48, 2011.
- [9] G. Paul, J. Philip, B. Raj and P. K. Das, “Indranil Manna, synthesis, characterization and thermal property measurement of nano-Al 95 Zn 05 dispersed nanofluid prepared by a two-step process,” *International Journal of Heat and Mass Transfer*, vol. 54, no. 15–16, pp. 3783–3788, 2011.

- [10] Y. Hwang, J. Lee, C. Lee, Y. Jung, S. Cheong, C. Lee, B. Ku and S. Jang, “Stability and thermal conductivity characteristics of nanofluids,” *Thermochimica Acta*, vol. 455, pp. 70–74, 2007.
- [11] X-J. Wang, D-S. Zhu and S. Yang, “Investigation of pH and SDBS on enhancement of thermal conductivity in nanofluids,” *Chemical Physics Letters*, vol. 470, pp. 107–111, 2009.
- [12] L. Yang, K. Du, X. S. Zhang and B. Cheng, “Reparation and stability of Al₂O₃ nano-particle suspension of ammonia–water solution,” *Applied Thermal Engineering*, vol. 31, pp. 3643–3647, 2011.
- [13] D. Anandan and K. Rajan, “Synthesis and stability of cupric oxide-based nanofluid: a novel coolant for efficient cooling,” *Asian Journal of Scientific Research*, vol. 5, no. 4, pp. 218–227, 2012.
- [14] . M. Chopkar, A. K. Das, I. Manna and P. K. Das, “Pool boiling heat transfer characteristics of ZrO₂-water nanofluids from a flat surface in a pool,” *Heat and Mass Transfer*, vol. 44, no. 8, pp. 999–1004, 2008.
- [15] L. Vekas, D. Bica and M. V. Avdeev, “Agnetic nanoparticles and concentrated magnetic nanofluids: synthesis, properties and some application,” *China Particuology*, vol. 5, pp. 43–49, 2007.
- [16] L. Véká, D. Bica and O. Marinica, “Magnetic nanofluids stabilized with various chain length surfactants,” *Romanian Reports in Physics*, vol. 58, no. 3, pp. 257–267, 2006.
- [17] S. U. S. Choi, “Nanofluids: from vision to reality through research,” *Journal of Heat Transfer*, vol. 131, 2009.
- [18] W. Yu and H. Xie, “A review on nanofluids: preparation, stability mechanisms and applications,” *Journal of Nanomaterials*, p. 17, 2012.
- [19] Malvern Instruments. *Technical Note: Zeta potential – an introduction in 30 minutes* Worcestershire, 2015.

- [20] R. Mondragon, J. Julia, A. Barba and J. Jarque, “Characterization of silica–water nanofluids dispersed with an ultrasound probe: a study of their physical properties and stability,” *Powder Technology*, vol. 224, no. 138–146, 2012.
- [21] M. Zawrah, R. Khattab, L. Girgis, H. E. Daidamony and R. E. Abdel Aziza, “Stability and electrical conductivity of water-base Al₂O₃ nanofluids for different applications,” *HBRC Journal*, 2015.
- [22] H. J. Kim, I. C. Bang and J. Onoe, “Characteristic stability of bare Au-water nanofluids fabricated by pulsed laser ablation in liquids,” *Optics and Lasers in Engineering*, vol. 47, no. 5, pp. 532–538, 2009.
- [23] J-H. Lee, K. S. Hwang, S. P. Jang, B. H. Lee, J. H. Kim, S. U. Choi and C. J. Choi, “Effective viscosities and thermal conductivities of aqueous nanofluids containing low volume concentrations of Al₂O₃ nanoparticles,” *International Journal of Heat and Mass Transfer*, vol. 51, no. 11–12, p. 2651–2656, 2008.
- [24] F. Fairuza and E. Zahir, “Analysis of optical spectrum for hematite nanofluid longpass tunable filter,” *American Journal of Engineering Research*, vol. 2, no. 12, pp. 126–130, 2013.
- [25] J. Huang, X. Wang, Q. Long, X. Wen, Y. Zhou and L. Li, “Influence of pH on the stability characteristics of nanofluids,” *Symposium on Photonics and Optoelectronics 2009*, 2009.
- [26] D. Zhu, X. Li, N. Wang, X. Wang, J. Gao and L. Hua, “Dispersion behavior and thermal conductivity characteristics of Al₂O₃–H₂O nanofluids,” *Current Applied Physics*, vol. 9, no. 1, pp. 131–139, 2009.
- [27] H. Zhu, C. Zhang, Y. Tang, J. Wang, B. Ren and Y. Yin, “Preparation and thermal conductivity of suspensions of graphite nanoparticles,” *Carbon*, vol. 45, no. 1, pp. 226–228, 2007.
- [28] V. W. Kaufui and D. L. Omar, “Applications of nanofluids: current and future,” *Advances in Mechanical Engineering*, 2010.

- [29] S. K. Das, S. U. S. Choi and H. E. Patel, “Heat transfer in nanofluids – a review,” *Heat Transfer Engineering*, vol. 27, no. 10, pp. 3–19, 2006.
- [30] S. J. Kim, I. C. Bang, J. Buongiorno and L. W. Hu, “Study of pool boiling and critical heat flux enhancement in nanofluids,” *Bulletin of the Polish Academy of Sciences – Technical Sciences*, vol. 55, no. 2, pp. 211–216, 2007.
- [31] D. Singh, J. Toutbort and G. Chen, “Heavy vehicle systems optimization merit review and peer evaluation,” *U.S. Department of Energy, Energy Efficiency and Renewable Energy* 2006.
- [32] M. J. Kao, C. Lo, T. T. Tsung, Y. Y. Wu, C. S. Jwo and H. M. Lin, “Copper oxide brake nanofluid manufactured using arcsubmerged nanoparticle synthesis system,” *Journal of Alloys and Compounds*, Vol. 434–435, pp. 672–674, 2007.
- [33] R. S. Shawgo, A. C. R. Grayson, Y. Li and M. J. Cima, “BioMEMS for drug delivery,” *Current Opinion in Solid State and Materials Science*, vol. 6, no. 4, pp. 329–334, 2002.
- [34] J. Buongiorno, “A benchmark study on the thermal conductivity of nanofluids,” *Journal of Applied Physics*, vol. 106, 2009.
- [35] W. Yu, D. M. France, J. L. Routbort and S. U. S. Choi, “Review and comparison of nanofluid thermal conductivity and heat transfer enhancements,” *Heat Transfer Engineering*, vol. 29, no. 5, pp. 432–460, 2008.
- [36] V. Trisaksri and S. Wongwises, “Critical review of heat transfer characteristics of nanofluids,” *Renewable and Sustainable Energy Reviews*, vol. 11, no. 3, pp. 512–523, 2007.
- [37] J. Eastman, S. Choi, S. Li, W. Yu and L. Thompson, “Anomalously increased effective thermal conductivities of ethylene glycol-based nanofluids containing copper nanoparticles,” *Applied Physics Letters*, vol. 78, no. 718, p. 718–720, 2001.
- [38] S. Das, N. Putra, P. Thiesen and W. Roetzel, “Temperature dependence of thermal conductivity enhancement for nanofluids,” *Journal of Heat Transfer*, vol. 125, no. 4, pp. 567–574, 2003.

- [39] S. Jana, A. Salehi-Khojin and W. Zhong, “Enhancement of fluid thermal conductivity by the addition of single and hybrid nano-additives,” *Thermochimica Acta*, vol. 462, pp. 45–55, 2007.
- [40] J. C. Maxwell, *A treatise on electricity and magnetism*, 2nd ed., Oxford: Clarendon, 1881.
- [41] D. Bruggeman, “Berechnung verschiedener physikalischer konstanten von heterogenen substanzen, I. Dielektrizitätskonstanten und Leitfähigkeiten der Mischkörper aus Isotropen Substanzen,” *Annalen der Physik*, vol. 24, pp. 636–679, 1935.
- [42] S. H. Kim, S. R. Choi and D. Kim, “Thermal conductivity of metal-oxide nanofluids: particle size dependence and effect of laser irradiation,” *Journal of Heat Transfer*, vol. 129, no. 3, pp. 298–307, 2006.
- [43] J. Jeong, C. Li, Y. Kwonb, J. Lee, S. H. Kim and R. Yun, “Particle shape effect on the viscosity and thermal conductivity of ZnO nanofluids,” *International Journal of Refrigeration*, vol. 36, no. 8, p. 2233–2241, 2013.
- [44] W. Yu and S. Choi, “The role of interfacial layers in the enhanced thermal conductivity of nanofluids: a renovated Maxwell model,” *Journal of Nanoparticle Research*, vol. 5, no. 1–2, pp. 167–171, 2003.
- [45] H. Ş. Aybar, M. Sharifpur, M. R. Azizian, M. Mehrabi and J. P. Meyer, “A review of thermal conductivity models for nanofluids,” *Heat Transfer Engineering*, vol. 36, no. 13, 2015.
- [46] L. Colla, L. Marinelli, L. Fedele, S. Bobbo and O. Manca, “Characterization and simulation of the heat transfer behaviour of water-based ZnO nanofluids,” *Journal of Nanoscience and Nanotechnology*, vol. 15, no. 5, pp. 3599–3609, 2015.
- [47] S. P. Jang and S. U. S. Choi, “Role of Brownian motion in the enhanced thermal conductivity of nanofluids,” *Applied Physics Letters*, vol. 84, no. 21, p. 4316–4318, 2004.
- [48] W. Yu, H. Xie, C. Lifei and Y. Li, “Investigation of thermal conductivity and viscosity of ethylene glycol based ZnO nanofluid,” *Thermochimica Acta*, vol. 491, no. 1–2, p. 92–96, 2009.

- [49] G. J. Lee, C. K. Kim, M. K. Lee, C. K. Rhee, S. Kim and C. Y. Kim, “Thermal conductivity enhancement of ZnO nanofluid using a one-step physical method,” *Thermochimica Acta*, vol. 542, pp. 24–27, 2012.
- [50] S. U. S. Choi, “Nanofluids: from vision to reality through research,” *Journal of Heat Transfer*, vol. 131, no. 3, 2009.
- [51] A. Einstein, *Investigations on the theory of the Brownian movement*, Courier Corporation, 1926.
- [52] H. C. Brinkman, “The viscosity of concentrated suspensions and solutions,” *Journal of Chemical Physics*, vol. 20, no. 4, p. 571–581, 1952.
- [53] K. Suganthi and K. Rajan, “Temperature induced changes in ZnO–water nanofluid: Zeta potential, size distribution and viscosity profiles,” *International Journal of Heat and Mass Transfer*, vol. 55, no. 25–26, p. 7969–7980, 2012.
- [54] B. C. Pak and Y. I. Cho, “Hydrodynamic and heat transfer study of dispersed fluids with submicron metallic oxide particles,” *Experimental Heat Transfer: A Journal of Thermal Energy Generation, Transport, Storage, and Conversion*, vol. 11, no. 2, pp. 151–170, 1998.
- [55] C. Nguyen, F. Desgranges, G. Roy, N. Galanis, T. Maré, S. Boucher and H. A. Mintsa, “Temperature and particle-size dependent viscosity data for water-based nanofluids – Hysteresis phenomenon,” *Heat and Mass Transfer*, vol. 28, no. 6, pp. 1492–1506, 2007.
- [56] S. Bobbo, L. Fedele, A. Benetti, L. Colla, M. Fabrizio, P. Cesare and S. Barison, “Viscosity of water based SWCNH and TiO₂ nanofluids,” *Experimental Thermal and Fluid Science*, vol. 36, pp. 65–71, 2012.

- [57] K. Anoop, T. Sundararajan and S. K. Das, “Effect of particle size on the convective heat transfer in nanofluid in the developing region,” *International Journal of Heat and Mass Transfer*, vol. 52, no. 9–10, pp. 2189–2195, 2009.
- [58] L. Godson, B. Raja, D. Mohan Lala and S. Wongwises, “Experimental investigation on the thermal conductivity and viscosity of silver-deionized water nanofluid,” *Experimental Heat Transfer: A Journal of Thermal Energy Generation, Transport, Storage and Conversion*, vol. 23, no. 4, pp. 317–332, 2010.
- [59] K. Khanafer and K. Vafai, “A critical synthesis of thermophysical characteristics of nanofluids,” *International Journal of Heat and Mass Transfer*, vol. 51, no. 19–20, p. 4410–4428, 2011.
- [60] R. S. Vajjha, D. K. Das and B. M. Mahagaonkar, “Density measurement of different nanofluids and their comparison with theory,” *Petroleum Science and Technology*, vol. 27, pp. 612–624, 2009.
- [61] A. Zaraki, M. Ghalambaz, A. J. Chamkha, M. Ghalambaz and D. D. Rossi, “Theoretical analysis of natural convection boundary layer heat and mass transfer of nanofluids: effects of size, shape and type of nanoparticles, type of base fluid and working temperature,” *Advanced Powder Technology*, 2015.
- [62] K. Khanafer, K. Vafai and M. Lightstone, “Buoyance-driven heat transfer enhancement in a two-dimensional enclosure utilizing nanofluid,” *International Journal of Heat and Mass Transfer*, vol. 46, p. 3639–3653, 2003.
- [63] E. J. Wasp, J. P. K. Kenny and R. L. Gandhi, “Solid–liquid flow slurry pipeline transportation,” *Trans Tech Publication*, 1977.
- [64] N. Putra, W. Roetzel and S. K. Das, “Natural convection of nanofluids,” *Heat and Mass Transfer*, vol. 39, no. 8, pp. 775–784, 2002.

- [65] K. S. Hwang, J. H. Lee and S. P. Jang, “Buoyancy-driven heat transfer of water-based Al_2O_3 nanofluids in a rectangular cavity,” *International Journal of Heat and Mass Transfer*, vol. 50, no. 19–20, p. 4003–4010, 2007.
- [66] S.P. Jang and S. U. S. Choi, “The role of Brownian motion in the enhanced thermal conductivity of nanofluids,” *Applied Physics Letters*, vol. 84, p. 4316–4318, 2004.
- [67] D. Wen and Y. Ding, “Formulation of nanofluids for natural convective heat transfer applications,” *International Journal of Heat and Fluid Flow*, vol. 26, no. 6, pp. 855–864, 2005.
- [68] C. Ho, M. Chen and Z. Li, “Numerical simulation of natural convection of nanofluid in a square enclosure: effects due to uncertainties of viscosity and thermal conductivity,” *International Journal of Heat and Mass Transfer*, vol. 51, no. 17–18, p. 4506–4516, 2008.
- [69] H. F. Oztopa and E. Abu-Nada, “Numerical study of natural convection in partially heated rectangular enclosures filled with nanofluids,” *International Journal of Heat and Fluid Flow*, vol. 29, no. 5, pp. 1326–1336, 2008.
- [70] A. K. Santra, S. Sen and N. Chakraborty, “Study of heat transfer augmentation in a differentially heated square cavity using copper–water nanofluid,” *International Journal of Thermal Sciences*, vol. 47, no. 9, pp. 1113–1122, 2008.
- [71] J. C. M. Garnett, “Colours in metal glasses and in metallic films,” *Philosophical Transactions of the Royal Society*, vol. 203, pp. 359–371, 1904.
- [72] E. B. Ögüt, “Natural convection of water-based nanofluids in an inclined enclosure with a heat source,” *International Journal of Thermal Sciences*, vol. 48, no. 11, p. 2063–2073, 2009.
- [73] C. Ho, W. Liu, Y. Chang and C. Lin, “Natural convection heat transfer of alumina-water nanofluid in vertical square enclosures: an experimental study,” *International Journal of Thermal Sciences*, vol. 49, no. 8, p. 1345–1353, 2010.

- [74] Z. Alloui, J. Guiet, P. Vasseur and M. Reggio, “Natural convection of nanofluids in a shallow rectangular enclosure heated from the side,” *The Canadian Journal of Chemical Engineering*, vol. 90, no. 1, pp. 69–78, 2012.
- [75] C. Qi, Y. He, S. Yan, F. Tian and Y. Hu, “Numerical simulation of natural convection in a square enclosure filled with nanofluid using the two-phase Lattice Boltzmann method,” *Nanoscale Research Letters*, vol. 8, 2013.
- [76] Y. Hu, Y. He, S. Wang, Q. Wang and H. I. Schlberg, “Experimental and numerical investigation on natural convection heat transfer of TiO₂-water nanofluids in a square enclosure,” *Journal of Heat Transfer*, vol. 136, no. 2, 2013.
- [77] C. Ho, D-S. Chen, W-M. Yan and O. Mahian, “Buoyancy-driven flow of nanofluids in a cavity considering the Ludwig–Soret effect and sedimentation: numerical study and experimental validation,” *International Journal of Heat and Mass Transfer*, vol. 77, pp. 684–694, 2014.
- [78] Y. Hu, Y. He, C. Qi, B. Jiang and H. I. Schlberg, “Experimental and numerical study of natural convection in a square enclosure filled with nanofluid,” *International Journal of Heat and Mass Transfer*, vol. 78, pp. 380–392, 2014.
- [79] U. Bhagat, P. More and P. Khanna, “Study of zinc oxide nanofluids for heat transfer application,” *South African Journal of Nanoscience and Nanotechnology*, vol. 1, no. 1, p. 101, 2015.
- [80] M. Sharifpur, H. Ghodsinezhad, J. Meyer and H. Rolfes, “Investigation on ultrasonic energy density effect on size distribution of zinc oxide (ZnO) nanoparticles by using zeta-sizer,” *Fluid Mechanics and Thermodynamics*, 2015.
- [81] Y. Hwang, J. Lee, C. Lee, Y. Jung, S. Cheong, C. Lee, B. Ku and S. Jang, “Stability and thermal conductivity characteristics of nanofluids,” *Thermochimica Acta*, vol. 455, pp. 70–74, 2007.

- [82] J. P. Konell, J. A. King and I. Mis, “Synergistic effects of carbon fillers on tensile and impact properties in nylon 6,6 and polycarbonate based resins,” *Polymer Composites*, vol. 25, no. 2, p. 172–185, 2004.
- [83] J. P. Konell, J. A. King and I. Miskioglu, “Synergistic effects of carbon fillers on tensile and impact properties in nylon 6,6 and polycarbonate based resins,” *Polymer Composites*, vol. 25, no. 2, pp. 172–185, 2004.
- [84] R. J. Moffat, “Describing the uncertainties in experimental results,” *Experimental Thermal and Fluid Science*, vol. 1, pp. 3–17, 1988.

Appendix A – Cavity design

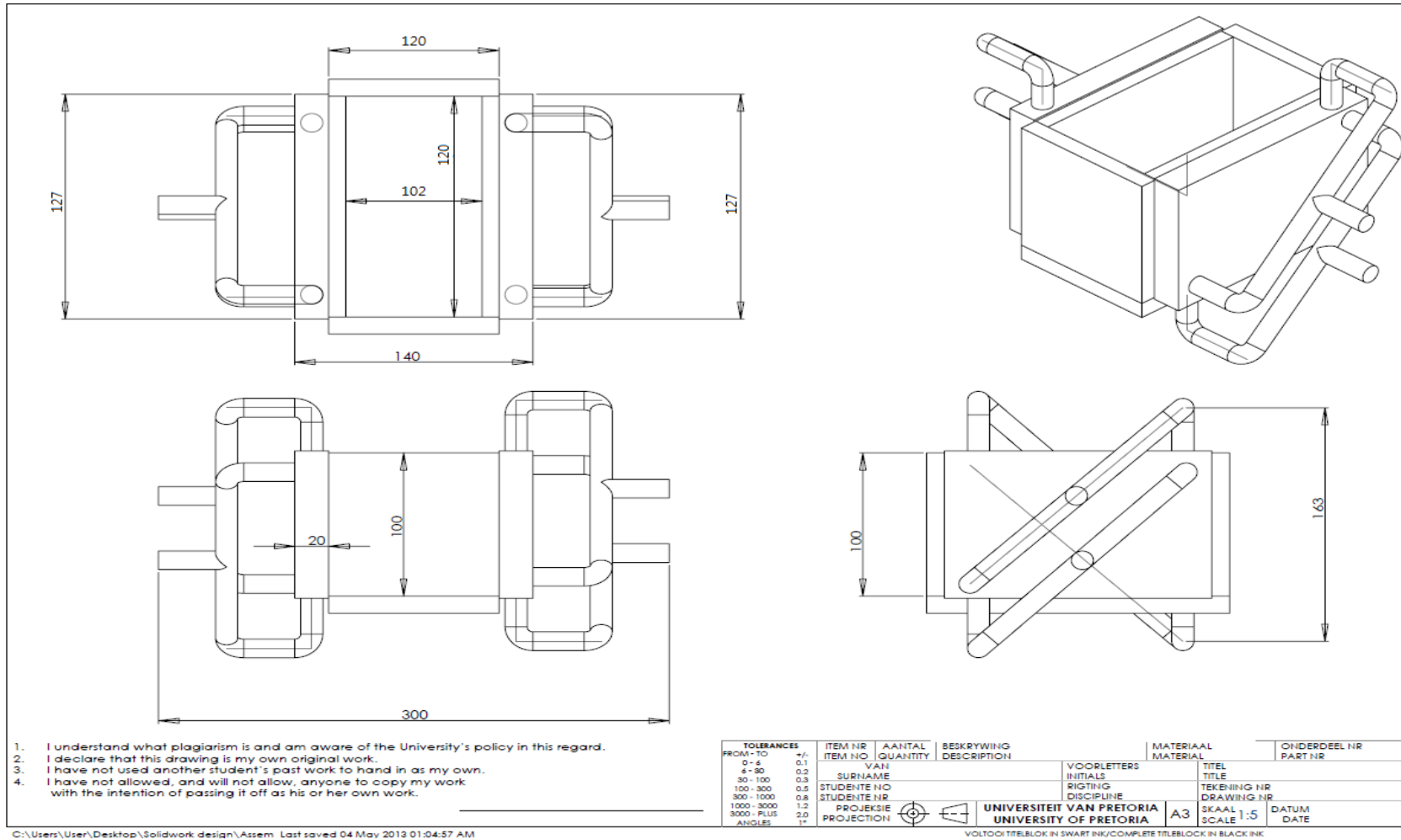


Figure A. 1: Test section dimensional drawings

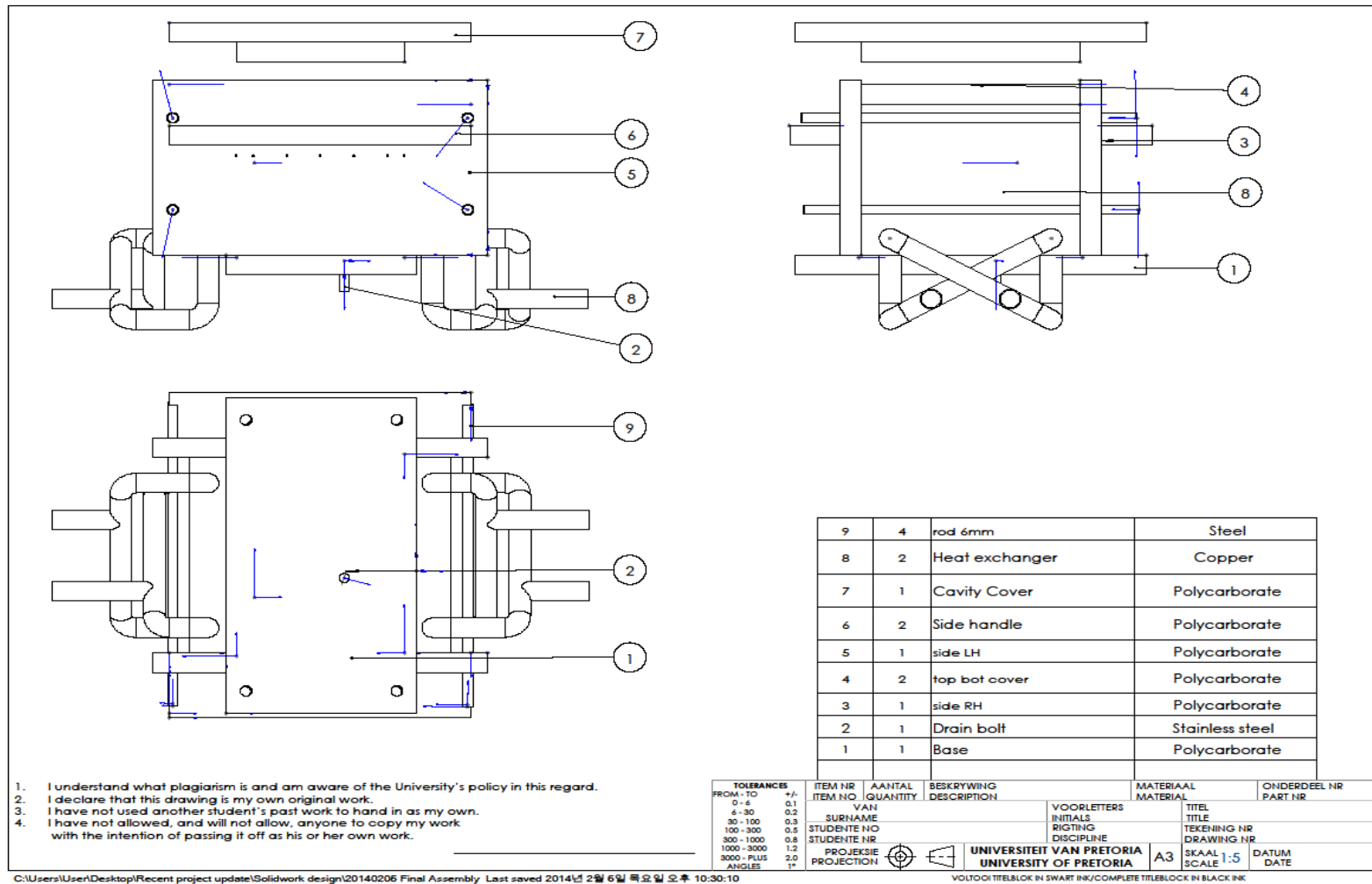


Figure A. 2: Test section drawing with bill of materials

Appendix B – Viscosity of ZnO-water nanofluid

Table B. 1: Viscosity of ZnO-water with volume concentration of (a) 0%, (b) 0.09%, (c) 0.18%, (d) 0.36%, (e) 0.5% and (f) 1%

Water only		0.09 vol.%	
Viscosity (mPa.s)	Temperature	Viscosity (mPa.s)	Temperature
1.23	10.00	1.20	9.99
1.08	14.98	1.03	14.99
0.95	20.01	0.90	20.00
0.85	25.00	0.80	25.01
0.77	30.01	0.71	29.99
0.69	35.03	0.64	34.99
0.64	40.02	0.58	40.00
0.59	45.04	0.54	45.00
0.56	50.02	0.50	50.05
0.54	54.98	0.47	55.02
0.53	60.05	0.45	59.98

(a)

(b)

0.18 vol.%		0.36 vol.%	
Viscosity (mPa.s)	Temperature	Viscosity (mPa.s)	Temperature
1.42	9.98	1.50	9.99
1.26	15.00	1.32	15.00
1.09	20.00	1.18	19.99
1.01	25.01	1.06	24.98
0.92	29.98	0.96	29.97
0.84	35.00	0.88	35.00
0.77	39.97	0.82	40.00
0.70	44.98	0.76	44.99
0.66	50.03	0.71	49.98
0.62	55.01	0.67	55.03
0.57	59.92	0.64	59.96

(c)

(d)

0.50 vol.%		1 vol.%	
Viscosity (mPa.s)	Temperature	Viscosity (mPa.s)	Temperature
1.41	9.99	1.58	10.00
1.23	14.98	1.35	15.00
1.09	20.00	1.21	20.00
0.98	25.01	1.10	25.01
0.89	30.00	0.99	30.01
0.80	35.00	0.88	35.00
0.75	40.00	0.82	40.00
0.69	45.01	0.75	45.01
0.63	49.97	0.71	50.03
0.59	54.94	0.69	55.02
0.55	60.02	0.67	59.81

(e)

(f)

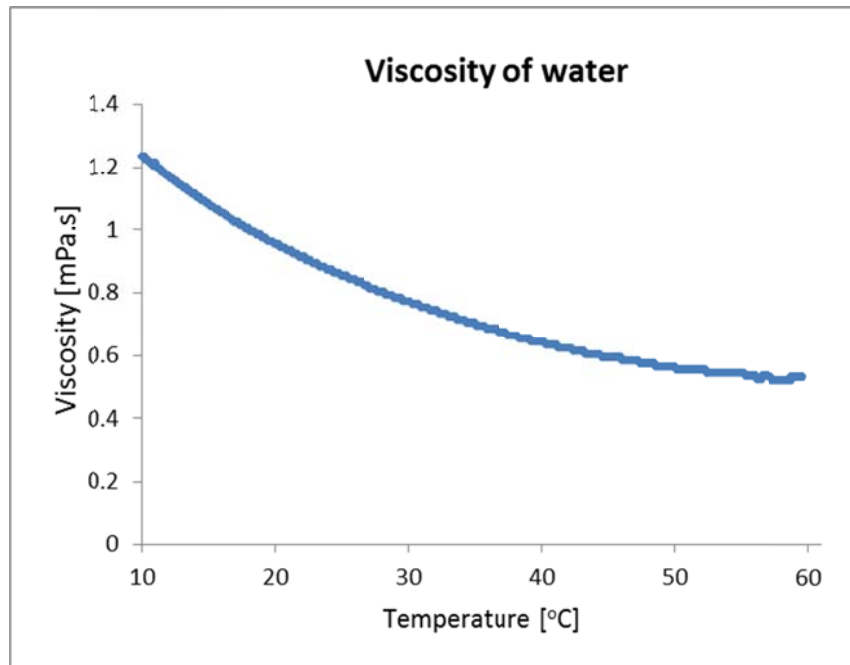


Figure B. 1: Viscosity of ZnO-water with 0% concentration as a function of temperature

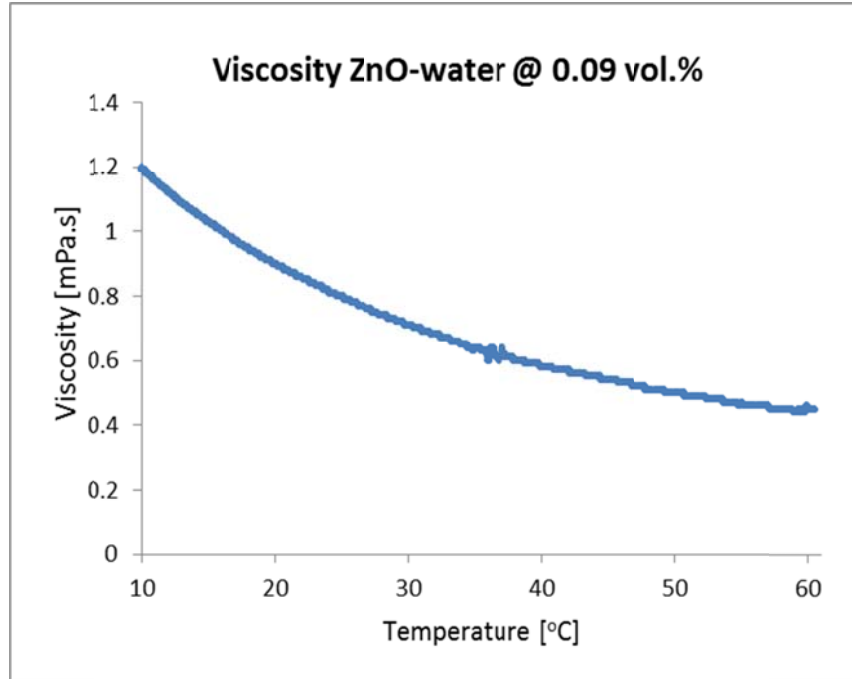


Figure B. 2: Viscosity of ZnO-water with 0.09% concentration as a function of temperature

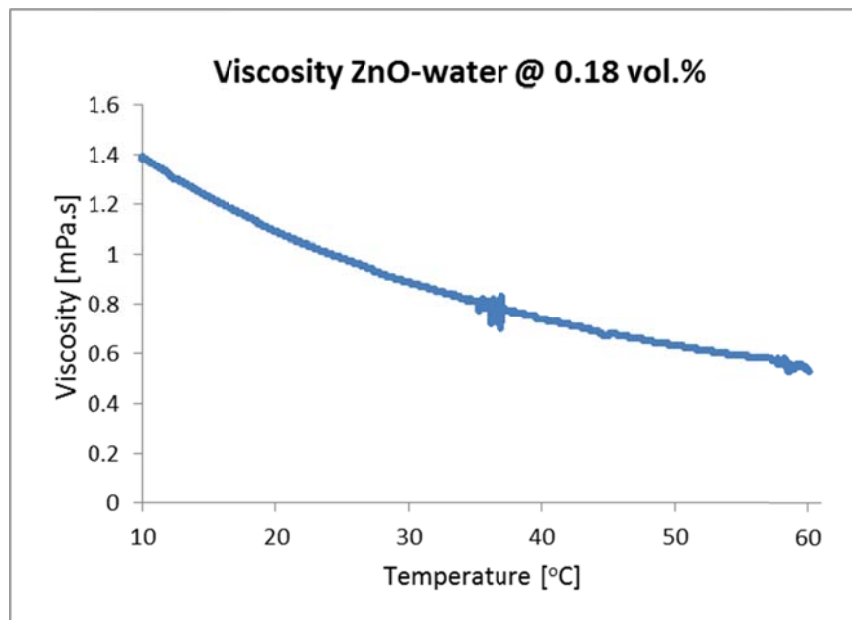


Figure B. 3: Viscosity of ZnO-water with 0.18% concentration as a function of temperature

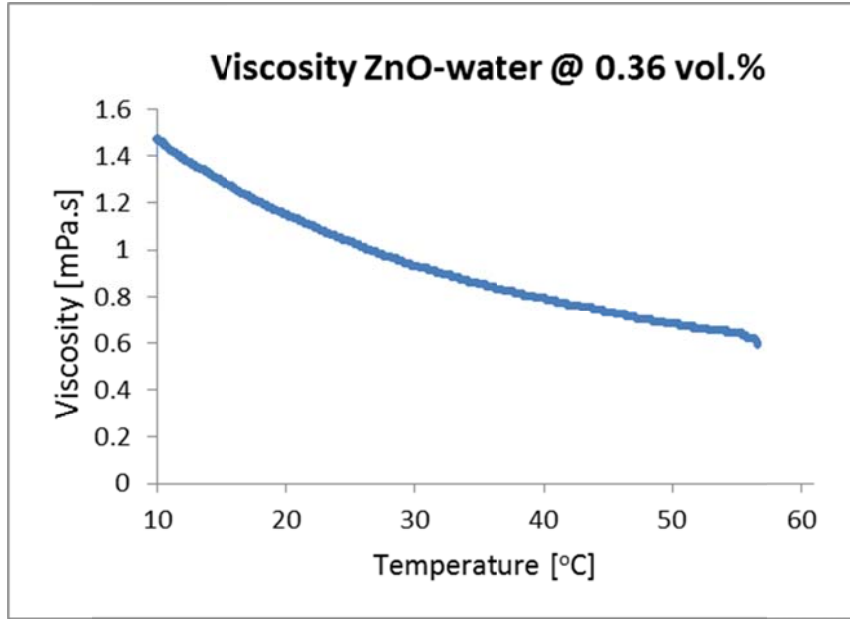


Figure B. 4: Viscosity of ZnO-water with 0.36% concentration as a function of temperature

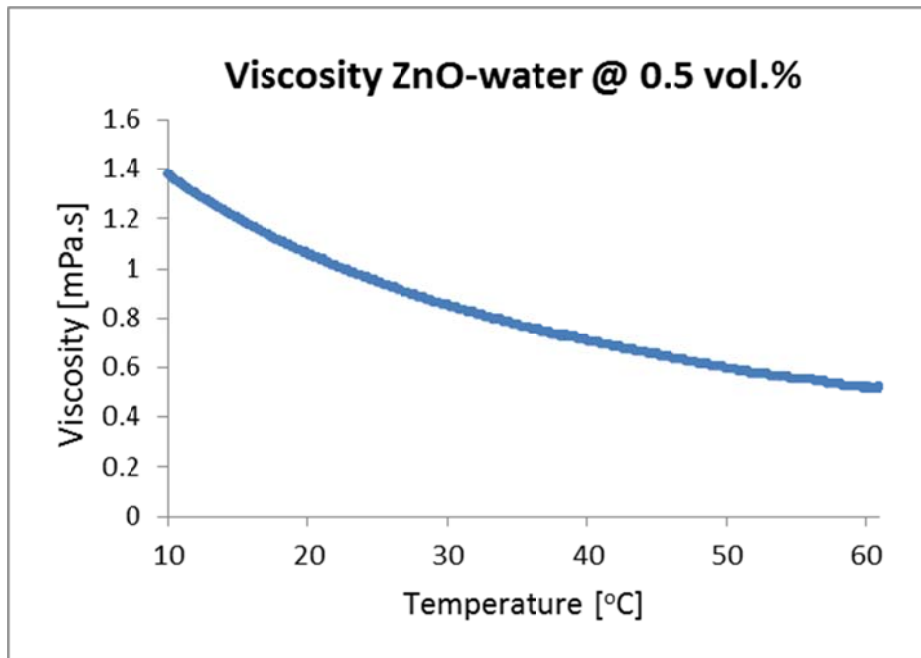


Figure B. 5: Viscosity of ZnO-water with 0.5% concentration as a function of temperature

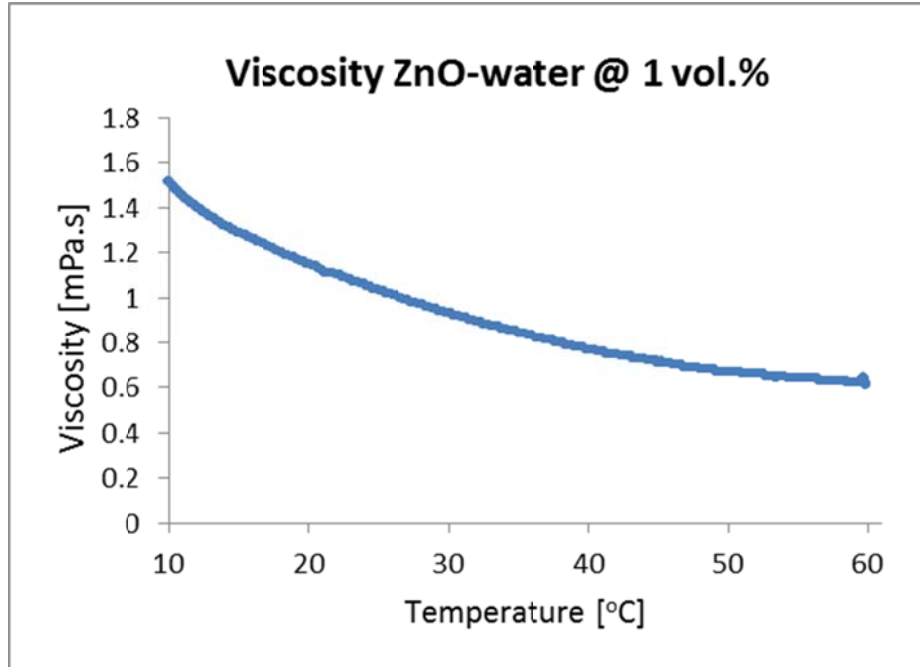


Figure B. 6: Viscosity of ZnO-water with 1% concentration as a function of temperature

Appendix C – Ra, Nu and heat transfer coefficient data

	Cold wall	9	9	10	6	3.1	5
Mass fraction	Hot wall	55	27	45	33	60	21
0 vol. %	Q Hot	112.54	36.83	80.13	51.51	133.66	26.99
	Q cold	110.98	28.32	77.23	50.86	148.00	23.53
	Q ave	111.7588857	32.57655416	78.67963398	51.18639142	140.8270793	25.26157801
	Ra	8.12E+08	1.50E+08	4.89E+08	2.53E+08	9.78E+08	8.82E+07
	h hot	405.22	308.57	380.33	300.48	409.64	248.85
	h cold	399.59	237.33	366.56	296.71	403.58	216.98
	h ave	402.4	273.0	373.4	298.6	406.6	232.9
	Nu hot	66.56	52.67	63.22	50.97	67.20	43.06
	Nu cold	65.63	40.51	60.93	50.33	74.41	37.55
Nu ave	66.09	46.59	62.07	50.65	70.81	40.30	
0.09 vol. %	Q Hot	110.78	32.22	80.44	47.02	129.24	24.94
	Q cold	110.40	30.96	76.83	51.13	149.42	24.44
	Q ave	110.59	31.59	78.63	49.08	139.33	24.69
	Ra	9.20E+08	1.75E+08	5.63E+08	2.71E+08	1.09E+09	9.72E+07
	h hot	379.43	250.37	348.65	264.55	368.51	215.44
	h cold	378.15	240.58	333.00	287.64	376.04	211.16
	h ave	3.79E+02	2.45E+02	3.41E+02	2.76E+02	3.72E+02	2.13E+02
	Nu hot	60.58	41.49	56.35	43.65	58.80	36.24
	Nu cold	60.38	39.86	53.82	47.46	67.98	35.52
Nu ave	60.48	40.67	55.08	45.56	63.39	35.88	
0.18 vol. %	Q Hot	114.47	34.59	81.32	49.42	132.65	24.89
	Q cold	112.71	31.11	76.54	42.50	128.71	24.92
	Q ave	113.59	32.85	78.93	45.96	130.68	24.91
	Ra	7.39E+08	1.44E+08	4.53E+08	2.36E+08	8.73E+08	8.58E+07
	h hot	386.99	266.44	348.75	276.22	375.05	210.04
	h cold	381.04	239.60	328.29	237.51	363.91	210.25
	h ave	3.84E+02	2.53E+02	3.39E+02	2.57E+02	3.69E+02	2.10E+02
	Nu hot	63.20	44.17	56.38	45.47	59.81	35.31
	Nu cold	62.23	39.72	53.07	39.10	58.03	35.34
Nu ave	62.72	41.95	54.72	42.29	58.92	35.32	
0.36 vol. %	Q Hot	111.23	36.62	79.47	48.19	133.44	25.96
	Q cold	111.56	26.96	77.31	51.15	147.62	14.65
	Q ave	111.39	31.79	78.39	49.67	140.53	20.30
	Ra	6.65E+08	1.31E+08	4.32E+08	2.16E+08	8.27E+08	8.71E+07
	h hot	381.25	276.87	340.89	268.74	376.17	218.19
	h cold	382.40	203.88	331.62	285.24	376.13	193.17
	h ave	381.82	240.37	336.26	276.99	376.15	205.68
	Nu hot	60.89	45.99	55.09	44.30	60.01	36.61
	Nu cold	61.08	33.86	53.59	47.02	66.39	20.66
Nu ave	60.98	39.93	54.34	45.66	63.20	28.64	
0.5 vol. %	Q Hot	106.74	32.07	78.46	46.24	128.95	24.13
	Q cold	114.99	31.87	77.56	51.01	150.18	25.68
	Q ave	110.87	31.97	78.01	48.62	139.57	24.91
	Ra	7.21E+08	1.48E+08	4.70E+08	1.96E+08	7.90E+08	7.45E+07
	h hot	368.23	247.27	341.01	256.81	364.74	203.25
	h cold	396.71	245.73	337.07	283.32	384.81	216.28
	h ave	382.47	246.50	339.04	270.06	374.77	209.77
	Nu hot	58.81	41.01	55.13	42.39	58.16	34.17
	Nu cold	63.36	40.76	54.49	46.77	67.74	36.37
Nu ave	61.08	40.88	54.81	44.58	62.95	35.27	
1 vol. %	Q Hot	108.98	32.41	75.25	47.97	133.33	19.02
	Q cold	98.62	31.02	75.93	41.77	124.47	29.55
	Q ave	103.80	31.72	75.59	44.87	128.90	24.29
	Ra	7.04E+08	1.89E+08	4.80E+08	2.25E+08	8.29E+08	1.39E+08
	h hot	372.05	244.05	317.07	261.19	379.62	158.64
	h cold	336.69	233.59	319.92	227.42	354.39	246.54
	h ave	354.37	238.82	318.50	244.31	367.00	202.59
	Nu hot	59.32	40.44	51.25	42.97	60.48	26.56
	Nu cold	53.68	38.70	51.71	37.42	56.46	41.28
Nu ave	56.50	39.57	51.48	40.20	58.47	33.92	

Table C. 1: Ra, Nu and heat transfer coefficient data

Appendix D – Uncertainty calculation

Equation of uncertainty analysis

$$\partial R = \left\{ \sum_{i=1}^N \left(\frac{\partial R}{\partial X_i} \partial X_i \right)^2 \right\}^{1/2}$$

$$\frac{\partial R}{R} = \left\{ \left(a \frac{\partial X_1}{X_1} \right)^2 + \left(b \frac{\partial X_2}{X_2} \right)^2 + \dots + \left(m \frac{\partial X_m}{X_m} \right)^2 \right\}^{1/2}$$

Uncertainty of heat transfer (Q_{hot})

$$\dot{Q} = \dot{m} C_{p,bf} (T_{in} - T_{out}) = \dot{m} C_{p,bf} T_{in} - \dot{m} C_{p,bf} T_{out}$$

$$\partial \dot{Q} = \left\{ \left(\frac{\partial \dot{Q}}{\partial \dot{m}} \partial \dot{m} \right)^2 + \left(\frac{\partial \dot{Q}}{\partial C_{p,bf}} \partial C_{p,bf} \right)^2 + \left(\frac{\partial \dot{Q}}{\partial T_{in}} \partial T_{in} \right)^2 \right\}^{1/2}$$

$$- \left\{ \left(\frac{\partial \dot{Q}}{\partial \dot{m}} \partial \dot{m} \right)^2 + \left(\frac{\partial \dot{Q}}{\partial C_{p,bf}} \partial C_{p,bf} \right)^2 + \left(\frac{\partial \dot{Q}}{\partial T_{out}} \partial T_{out} \right)^2 \right\}^{1/2}$$

$$\partial \dot{Q} = 3.163 \text{ W}$$

$$\frac{\partial \dot{Q}}{\dot{Q}} = \frac{3.163}{108} = 2.93\%$$

Uncertainty of heat transfer coefficient (h)

$$h_{nf} = \frac{\dot{Q}}{HW(T_H - T_C)}$$

$$\partial h_{nf} = \left\{ \left(\frac{\partial h}{\partial \dot{Q}} \partial \dot{Q} \right)^2 + \left(\frac{\partial h}{\partial H} \partial H \right)^2 + \left(\frac{\partial h}{\partial W} \partial W \right)^2 + \left(\frac{\partial h}{\partial T_H} \partial T_H \right)^2 + \left(\frac{\partial h}{\partial T_C} \partial T_C \right)^2 \right\}$$

$$\partial h_{nf} = 10.835$$

$$\frac{\partial h_{nf}}{h_{nf}} = 3.06\%$$

Uncertainty of Nu

$$Nu_{nf} = \frac{h_{nf} L_c}{k_{nf}}$$

$$\partial \text{Nu}_{\text{nf}} = \left\{ \left(\frac{\partial \text{Nu}_{\text{nf}c}}{\partial h_{\text{nf}}} \partial h_{\text{nf}} \right)^2 + \left(\frac{\partial \text{Nu}_{\text{nf}c}}{\partial L_c} \partial L_c \right)^2 + \left(\frac{\partial \text{Nu}_{\text{nf}c}}{k_{\text{nf}}} k_{\text{nf}} \right)^2 \right\}^{1/2}$$

$$\frac{\partial \text{Nu}_{\text{nf}}}{\text{Nu}_{\text{nf}}} = 3.056\%$$

Uncertainty of Ra

$$\text{Ra}_{\text{nf}} = \frac{g \beta_{\text{nf}} \rho_{\text{nf}}^2 L_c^3 (T_H - T_C)}{\mu_{\text{nf}} k_{\text{nf}}}$$

$$\begin{aligned} \partial \text{Ra}_{\text{nf}} = & \left\{ \left(\frac{\partial \text{Ra}_{\text{nf}}}{\partial \beta_{\text{nf}}} \partial \beta_{\text{nf}} \right)^2 + \left(\frac{\partial \text{Ra}_{\text{nf}}}{\partial \rho_{\text{nf}}} \partial \rho_{\text{nf}} \right)^2 + \left(\frac{\partial \text{Ra}_{\text{nf}}}{\partial L_c} \partial L_c \right)^2 + \left(\frac{\partial \text{Ra}_{\text{nf}}}{\partial T_H} \partial T_H \right)^2 + \left(\frac{\partial \text{Ra}_{\text{nf}}}{\partial T_L} \partial T_L \right)^2 \right. \\ & \left. + \left(\frac{\partial \text{Ra}_{\text{nf}}}{\partial \mu_{\text{nf}}} \partial \mu_{\text{nf}} \right)^2 + \left(\frac{\partial \text{Ra}_{\text{nf}}}{\partial k_{\text{nf}}} \partial k_{\text{nf}} \right)^2 \right\}^{1/2} \end{aligned}$$

$$\frac{\partial \text{Ra}_{\text{nf}}}{\text{Ra}_{\text{nf}}} = 4.36\%$$